



THE FABRICATION AND CHARACTERIZATION OF MULTIFUNCTIONAL  
TiO<sub>2</sub> - EMBEDDED - CROSSLINKED CHITOSAN MICROBEADS FOR  
PHOTOCATALYTIC AND ADSORBENT PROPERTIES

BY

MR. THUNPICHET OONESIRITHUPSAKUL

A THESIS SUBMITTED IN PARTIAL FULFILLMENT OF THE REQUIREMENTS FOR  
THE DEGREE OF MASTER OF SCIENCE (CHEMISTRY)

DEPARTMENT OF CHEMISTRY

FACULTY OF SCIENCE AND TECHNOLOGY

THAMMASAT UNIVERSITY

ACADEMIC YEAR 2017

COPYRIGHT OF THAMMASAT UNIVERSITY

THE FABRICATION AND CHARACTERIZATION OF MULTIFUNCTIONAL  
TiO<sub>2</sub> - EMBEDDED - CROSSLINKED CHITOSAN MICROBEADS FOR  
PHOTOCATALYTIC AND ADSORBENT PROPERTIES

BY

MR. THUNPICHET OONESIRITHUPSAKUL



A THESIS SUBMITTED IN PARTIAL FULFILLMENT OF THE REQUIREMENTS FOR  
THE DEGREE OF MASTER OF SCIENCE (CHEMISTRY)

DEPARTMENT OF CHEMISTRY

FACULTY OF SCIENCE AND TECHNOLOGY

THAMMASAT UNIVERSITY

ACADEMIC YEAR 2017

COPYRIGHT OF THAMMASAT UNIVERSITY

THAMMASAT UNIVERSITY  
FACULTY OF SCIENCE AND TECHNOLOGY

THESIS

BY

MR. THUNPICHET OONESIRITHUPSAKUL

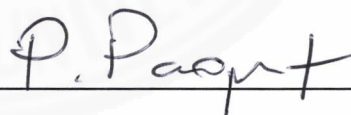
ENTITLED

THE FABRICATION AND CHARACTERIZATION OF MULTIFUNCTIONAL  
TiO<sub>2</sub> - EMBEDDED - CROSSLINKED CHITOSAN MICROBEADS FOR PHOTOCATALYTIC AND  
ADSORBENT PROPERTIES

was approved as partial fulfillment of the requirements for  
the Degree of Master of Science (Chemistry)

on July 26<sup>th</sup>, 2018

Chairman



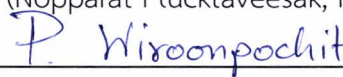
(Associate Professor Peerasak Paoprasert, Ph.D.)

Advisor



(Nopparat Plucktaveesak, Ph.D.)

Member



(Panithi Wiroonpochit, Ph.D.)

Dean



(Associate Professor Somchai Chakhatrakan, Ph.D.)

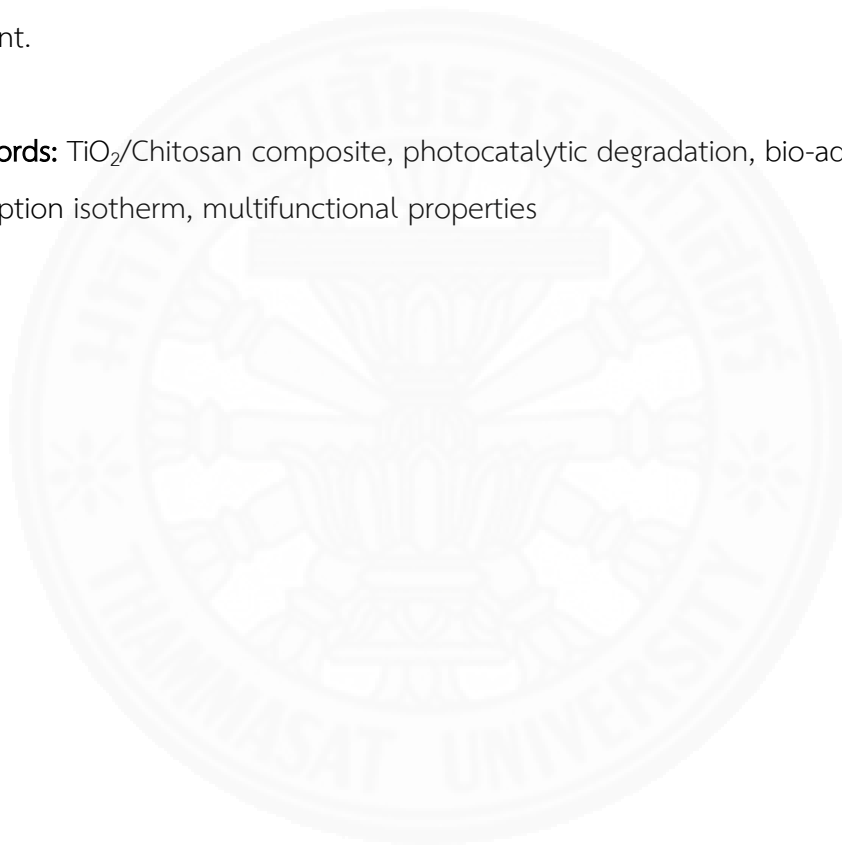
Thesis Title	THE FABRICATION AND CHARACTERIZATION OF MULTIFUNCTIONAL TiO <sub>2</sub> - EMBEDDED - CROSSLINKED CHITOSAN MICROBEADS FOR PHOTOCATALYTIC AND ADSORBENT PROPERTIES
Author	Mr. Thunpichet Oonsirithupsakul
Degree	Master of Science (Chemistry)
Department/Faculty/University	Department of Chemistry Faculty of Science and Technology Thammasat University
Thesis Advisor	Nopparat Plucktaveesak, Ph.D.
Academic Year	2017

## ABSTRACT

The fabrication of TiO<sub>2</sub> - embedded – cross-linked chitosan microbeads was successfully prepared. The obtained TiO<sub>2</sub>/Chitosan composite possesses multifunctional properties i.e., to serve as a bio-adsorbent for the removal of toxic metal ions and also as a photocatalyst in the degradation of organic contaminants. Therefore the aim of this composite is to use in wastewater treatment especially in textile industry where both of its functions can be utilized. To characterize the photocatalytic property, the decomposition of indigo carmine under UV radiation was employed. It was found that the model dye was decomposed up to 85.91% within 36 hours when 2 g of 3 wt% - TiO<sub>2</sub>/Chitosan composite was used. The time required to completely degrade the dye depended not only on the percentage of TiO<sub>2</sub> embedded, but also on the amount of composite used as well. The more the composite added, the faster the degradation process occurs. Moreover, the recyclability of this photo-catalyst was also determined. The results showed that this composite still maintained its photocatalytic efficiency even after three times of reuse, when epichlorohydrin was used as crosslinking agent. Furthermore, the

adsorption and desorption behavior characteristics of the prepared composite were investigated. The adsorption-desorption isotherm of Cr (VI) ions commonly found in textile industry, of this composite was studied. The maximum Cr (VI) adsorption capacity was achieved at  $398.5 \text{ mg}\cdot\text{g}^{-1}$ . The results indicated the potential applications of the prepared  $\text{TiO}_2/\text{Chitosan}$  composite to be used as photo-catalyst and bio-adsorbent. This multifunctional composite is suitable for wastewater treatment in textile industry where both organic compounds and toxic metal ions are present.

**Keywords:**  $\text{TiO}_2/\text{Chitosan}$  composite, photocatalytic degradation, bio-adsorbent, adsorption isotherm, multifunctional properties



## ACKNOWLEDGEMENTS

The author wishes to sincerely express his profound thanks and gratitude to those individual and organization that provide their valuable support and assistance in the completion of his master degree.

First and foremost, his thanks go to his supervisor, Dr. Nopparat Plucktaveesak for the encouraging guidance, supervision, valuable suggestions and enthusiastic support throughout this research.

The author also would like to acknowledge Assoc. Prof. Dr. Peerasak Paoprasert and Dr. Panithi Wiroonpochit, for their participation as the dissertation chairman and member of thesis committee, respectively.

To the Department of Chemistry, Faculty of Science and Technology, Thammasat University for giving the opportunity to pursue his research to a success and providing the excellent laboratory facilities and instrument used in this research. Moreover, thanks for its partial financial support, so he could attend his first international conference i.e., the MRS-Thailand 2017 International Conference.

To Human Resource Development in Science Project (Science Achievement Scholarship of Thailand, SAST) for providing the scholarship to pursue his Master's Degree study in this institution.

A warm thanks is expressed to his entire friends in the laboratory for their friendship and helps during the course of his graduate research.

Finally, the author would like to express his deep appreciation to his family for their love, support and endless encouragement throughout his entire study.

Mr. Thunpichet Oonesirithapsakul

## TABLE OF CONTENTS

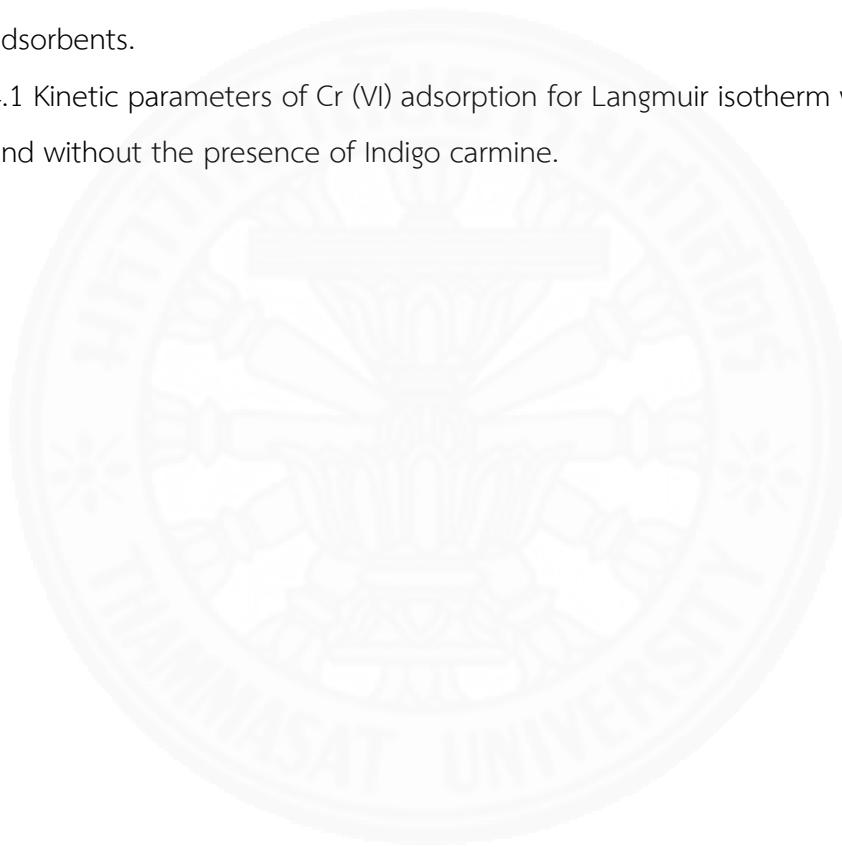
	Page
ABSTRACT	(1)
ACKNOWLEDGEMENTS	(3)
LIST OF TABLES	(6)
LIST OF FIGURES	(7)
LIST OF ABBREVIATIONS	(9)
CHAPTER 1 INTRODUCTION	1
1.1 The Purpose of the Investigation	1
1.2 Objective	3
1.3 Scope of the investigation	3
CHAPTER 2 REVIEW OF LITERATURE	4
2.1 Titanium dioxide as a photocatalyst	4
2.2 The principle of photocatalytic mechanism and dye degradation	4
2.2.1 Indirect dye degradation mechanism	4
2.2.2 Direct dye degradation mechanism	6
2.3 Heavy metal adsorption isotherm	7
2.4 Literature reviews	8

CHAPTER 3 RESEARCH METHODOLOGY	10
3.1 Material	10
3.1.1 Chemicals	10
3.1.2 Equipment	10
3.2 Preparation of TiO <sub>2</sub> /Chitosan microbeads with crosslinking agents	11
3.3 Dye decomposition experiment and analysis	12
3.4 Heavy metal adsorption experiment and analysis	13
3.5 Multifunctional property experiment and analysis	15
CHAPTER 4 RESULTS AND DISCUSSION	18
4.1 The photodegradation of TiO <sub>2</sub> rutile powders	18
4.2 The photodegradation of Indigo carmine with TiO <sub>2</sub> /Chitosan microbeads	19
4.2.1 Effect of the amount of TiO <sub>2</sub> microbeads on the photodegradation of Indigo carmine	19
4.2.2 Effect of crosslinking agents used to strengthen the microbeads on the photodegradation of Indigo carmine	20
4.2.3 The study of recyclability of the TiO <sub>2</sub> /chitosan microbeads	22
4.2.4 The optical microscope image of microbeads with various crosslinking agents	25
4.3 The Cr (VI) adsorption isotherm of TiO <sub>2</sub> /Chitosan microbeads	27
4.4 Multifunctional properties of TiO <sub>2</sub> /Chitosan microbeads	30
CHAPTER 5 CONCLUSIONS	32
REFERENCES	34
BIOGRAPHY	40



## LIST OF TABLES

Tables	Page
2.1 The comparison of dye degradation with various methods by using TiO <sub>2</sub> photocatalyst	8
2.2 The comparison of heavy metal adsorption with various adsorbents.	9
4.1 Kinetic parameters of Cr (VI) adsorption for Langmuir isotherm with and without the presence of Indigo carmine.	27



## LIST OF FIGURES

Figures	Page
2.1 Pictorial representation of indirect dye degradation process	5
2.2 Pictorial representation of direct dye degradation process	6
3.1 The preparation of TiO <sub>2</sub> /Chitosan microbeads	11
3.2 The Dye decomposition experiment	12
3.3 The heavy metal adsorption experiment	14
3.4 The study of multifunctional properties	16
4.1 The percentage of photodegradation of 10 ppm Indigo carmine solution using 0.3 g of TiO <sub>2</sub> powder.	18
4.2 The effect of the amount of beads used on the decomposition of dye.	19
4.3 The photodegradation of dye with 2 g of 1, 3 and 5 wt% of TiO <sub>2</sub> embedded into chitosan microbeads cross-linked with glutaraldehyde	21
4.4 The photodegradation of dye with 2 g of 3 and 5 wt% of TiO <sub>2</sub> embedded into chitosan microbeads and cross-linked with epichlorohydrin (ECH).	22
4.5 The recyclability of 2 g of 3wt% TiO <sub>2</sub> /Chitosan microbeads cross-linked with 0.1 M epichlorohydrin and ran by 16 gauge needle size.	24
4.6 The recyclability of 2 g of 3wt% TiO <sub>2</sub> /Chitosan microbeads cross-linked with 0.5 M epichlorohydrin and ran by 16 gauge needle size.	24
4.7 The recyclability of 2 g of 3wt% TiO <sub>2</sub> /Chitosan microbeads cross-linked with 0.1 M epichlorohydrin and ran by 20 gauge needle size.	25
4.8 The microscopic image of 3 wt% TiO <sub>2</sub> /Chitosan cross-linked with Glutaraldehyde crosslinking agent.	26
4.9 The microscopic image of 3 wt% TiO <sub>2</sub> /Chitosan cross-linked with Epichlorohydrin crosslinking agent.	26
4.10 Langmuir isotherms of Cr (VI) ions with TiO <sub>2</sub> /Chitosan microbeads	28

without the presence of Indigo carmine.

4.11 Langmuir isotherms of Cr (VI) ions with TiO<sub>2</sub>/Chitosan microbeads 29

with the presence of Indigo carmine.

4.12 Langmuir isotherms of Cr (VI) ions with TiO<sub>2</sub>/Chitosan microbeads 29

with and without the presence of Indigo carmine on the same plot

4.13 The multifunctional properties of TiO<sub>2</sub>/Chitosan microbeads 31

soaked into the solution containing of both Cr (VI) ions and Indigo carmine.



## LIST OF ABBREVIATIONS

Symbols/Abbreviations	Terms
$C_e$	Equilibrium concentration of solute remaining in solution
$\theta$	Surface coverage
ECH	Epichlorohydrin
IC	Indigo carmine
ICP-OES	Inductively coupled plasma–optical emission spectrometry
$K_{ads}$	Equilibrium constant
$q_e$	Amount of solute adsorbed per unit weight of solid at equilibrium
$q_{max}$	Maximum adsorption capacity for forming single layer

## CHAPTER 1

### INTRODUCTION

#### 1.1 The Purpose of the Investigation

The residual dyes from different sources of industries (e.g., textile industries, paper and pulp industries, dye intermediates industries, pharmaceutical industries, tannery, and Kraft bleaching industries, etc.) are widely taking into consideration due to their toxicity. They are needed to be treated to remove those toxic contaminants before discharging into natural resources [1-3].

Under the UV light or even normal light, these organic dyes can be decomposed naturally but the process takes such a long time, which is not practical and could not be waited. Various techniques and modifications have been used to speed up this process. The simple and widely accepted technique is the use of photocatalyst, especially the use of Titania ( $\text{TiO}_2$ ) for this purpose [4-6]. It has been widely used in the photocatalytic decomposition of organic dyes due to its chemically stable and harmless. The larger band gap, which is about 3.0 eV and 3.2 eV for those forms of  $\text{TiO}_2$  namely rutile and anatase, respectively makes this catalyst primarily active under the exposure of UV radiation [7].

In addition to organic dye contaminants, heavy metal ions such as Cr (VI), Cu (II) and Cd (II) ions are also commonly found in wastewater collected from textile industry. This type of contaminants is also considered as a threat to the environment. Therefore, any treatment that can tackle these two issues at the same time would be more suitable. It has been known that many bio-sorbents such as chitosan, and sugarcane bagasse have the ability to adsorb those heavy metal ions to some extents. So, the combination of  $\text{TiO}_2$  and bio-sorbent could solve those two issues mentioned above.

In this study, the system containing  $\text{TiO}_2$  and chitosan were considered. Chitosan was chosen due to its abundance, low cost, nontoxic and biodegradable [10]. It is derived from various natural sources including exoskeleton of insects,

crustacean such as crabs and shrimps, and cell walls of some fungi [11]. Chitosan, the  $\beta$ -(1,4)-linked polysaccharide of D-glucosamine, is a cationic biopolymer containing two free and active functional groups i.e., hydroxyl and amine groups. These two functional groups are also readily available for crosslinking [12-20]. The most commonly used crosslinking agents include glutaraldehyde, epichlorohydrin and triphosphate [21-26].

In this study, the fabrication of TiO<sub>2</sub> embedded-cross-linked chitosan microbeads was considered. With the two active species, this composite could tackle two issues found in the treatment of wastewater collected from the textile industry. Under the exposure of UV radiation, the TiO<sub>2</sub> particles can act as the photocatalyst to speed up the photodegradation process of organic dye contaminants. At the same time, with the presence of chitosan, heavy metal ions such as Cr (VI) and Cu (II) can be removed from the wastewater. The microbeads was chosen as the form of these active ingredients instead of powder form due to their ease to be recovered after usage. Therefore multiple uses of these microbeads were also taken into consideration. To be able to be repeatedly use these microbeads without any treatment, their stability under acidic condition needed to strengthen. By crosslinking the chitosan molecules to some degrees, the microbeads become more stable and could be used repeatedly.

## 1.2 Objective

1.2.1 To optimize the condition for the decomposition of the Indigo carmine using TiO<sub>2</sub>/chitosan microbeads.

1.2.2 To investigate the recyclability of TiO<sub>2</sub>/Chitosan microbeads as the photocatalyst and bio-adsorbent for the treatment of wastewater containing Indigo carmine and Cr (VI) ions.

1.2.3 To study the adsorption of Cr (VI) ions of the prepared TiO<sub>2</sub>/Chitosan microbeads.

1.2.4 To study the effect of Cr (VI) ions on the decomposition of Indigo carmine.

## 1.3 Scope of the investigation

1.3.1 Only 2 wt% chitosan solution was studied. It was found to be the most suitable concentration to easily form microbeads.

1.3.2 Three amounts of loaded TiO<sub>2</sub> particles (rutile form) including 1, 3 and 5 wt% were varied.

1.3.3 Two of crosslinking agents i.e., glutaraldehyde and epichlorohydrin with two concentrations, which were 0.1 and 0.5 M were investigated.

1.3.4 To form microbeads, two needle size were used i.e., 16 and 20 gauge sizes.

1.3.4 The model wastewater was prepared and used throughout this study containing 1000 ppm of Cr (VI) ions and 100 ppm of Indigo carmine.

## CHAPTER 2

### THEORY AND LITERATURE REVIEW

#### 2.1 Titanium dioxide as a photocatalyst

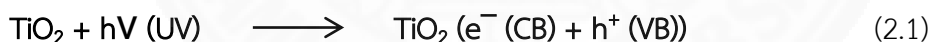
Among commonly known photocatalysts, Titanium dioxide (TiO<sub>2</sub>) has been widely used and studied due to its non-toxicity, high stability and strong oxidizing power [27]. Its large band gap enables it to be excited by UV light with the wavelength below 415 nm or 385 nm in its rutile and anatase phase, respectively [28-34]. The only drawback of using TiO<sub>2</sub> seems to be its limitation to be used within the UV range. Therefore under normal light, its effectiveness is limited [31-34].

#### 2.2 The principle of photocatalytic mechanism and dye degradation

##### 2.2.1 Indirect dye degradation mechanism

The indirect heterogeneous photocatalytic oxidation mechanism using semiconducting materials can be summarized as follows.

##### *Photoexcitation*



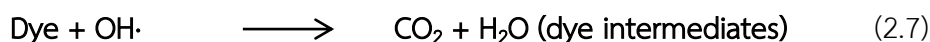
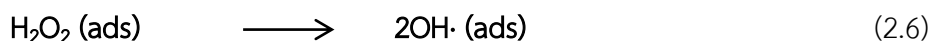
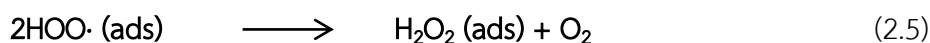
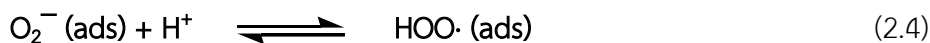
##### *Ionized of water*



##### *Oxygen ionosorption*



##### *Protonation of superoxide*





Photocatalytic reaction is initiated when a photoelectron is excited from the filled valence band to the empty conduction band as a result of UV radiation. The excitation process leaves behind a hole in the valence band ( $h^+$  (VB)). As a result, electron and hole pair ( $e^-/h^+$ ) is generated.

Then the photogenerated holes react with water to produce hydroxyl radicals ( $OH\cdot$ ). The  $HO\cdot$  radicals formed on the surface of  $TiO_2$  particle are extremely powerful oxidizing agent. It attacks adsorbed organic molecules causing them to decompose to some extents depending on their structure and stability.

While the photogenerated hole ( $h^+$  (VB)) reacts with  $OH^-$  to produce the hydroxyl radical, electron in the conduction ( $e_{CB}^-$ ) is taken up by the oxygen to generate anionic superoxide radical ( $O_2^-$ ). This superoxide ion not only takes part in the oxidation process but also prevents the electron-hole recombination, therefore maintaining electron neutrality within the  $TiO_2$  molecule.

The superoxide ( $O_2^-$ ) produced gets excited forming hydroperoxyl radical ( $HO_2\cdot$ ) and then subsequently  $H_2O_2$ . The peroxide then dissociates into highly reactive hydroxyl radicals ( $OH\cdot$ ). These reactions of oxidation and reduction processes commonly take place on the surface of the photoexcited photocatalyst as shown in Figure 2.1 [35].

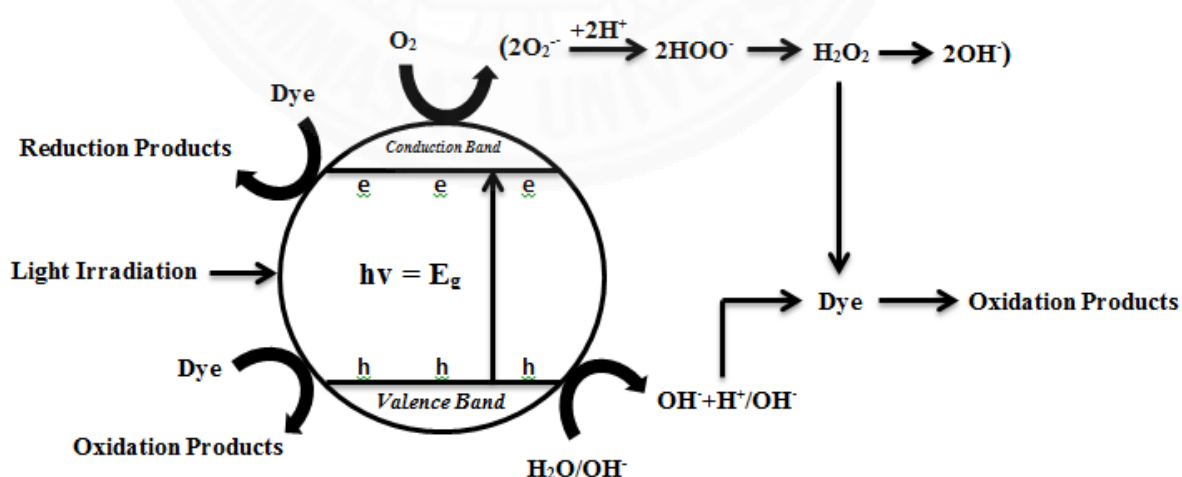


Figure 2.1 Pictorial representation of indirect dye degradation process [35].

### 2.2.2 Direct dye degradation mechanism

Another mechanism of photocatalytic dye degradation can also occur under visible light since it can adsorb visible light as well. This mechanism involves the dye excitation to the triplet excited state (Dye<sup>\*</sup>). This excited state dye species is then converted into a semi-oxidized radical cations (Dye<sup>+</sup>). Due to reaction between these trapped electrons and oxygen in the system, the superoxide radical anions (O<sub>2</sub><sup>-</sup>) are formed. These anions later turn into hydroxyl radicals (OH<sup>·</sup>). These OH<sup>·</sup> radicals are mainly responsible for the decomposition of the organic compounds [35].

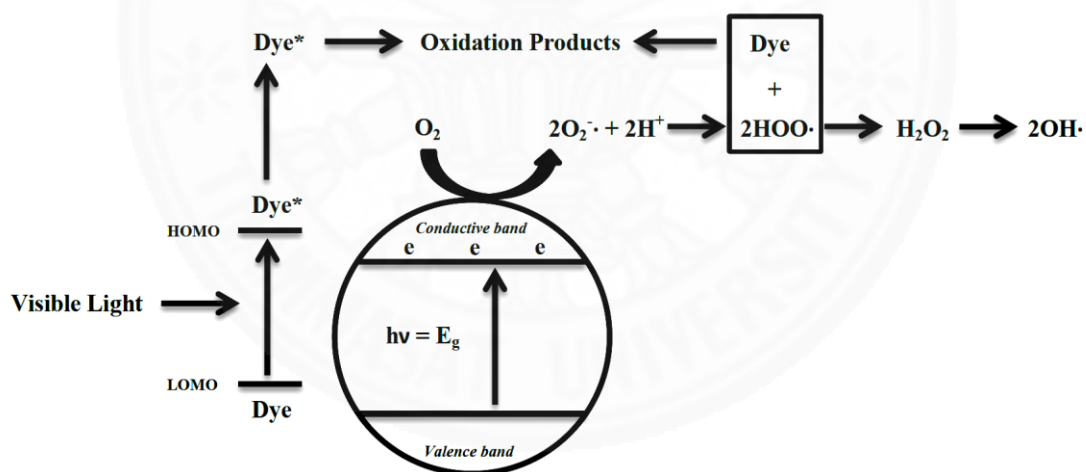


Figure 2.2 Pictorial representation of direct dye degradation process [35].

## 2.3 Heavy metal adsorption isotherm

Chromium and its compounds are commonly found in plating, leather tanning, dye, cement, and photography industries and considered as toxic pollutants [36]. Two forms of Chromium ions include trivalent and hexavalent are considered as environment threat [37]. By using adsorbent, these heavy metal ions could be removed through the adsorption process. Adsorption is technique suitable for the removal of low concentrations of pollutants from large volumes contaminated water. Its equilibrium information is important to understand of how much ions can be adsorbed by a solid adsorbent [38]. Adsorption isotherm is used to describe how heavy metal ions interact with adsorbent materials such as chitosan with relate to adsorption properties and equilibrium data.

For solid – liquid adsorption system, at equilibrium, a saturation point or the maximum adsorption is reached where no further adsorption can occur. The important of adsorption isotherm is to represent the relationship between the mass of adsorbate adsorbed per unit weight of adsorbent and the liquid-phase equilibrium concentration of adsorbate [39].

One of the well-accepted model of adsorption isotherm is Langmuir's isotherm describing the adsorption of adsorbate (A) onto the surface of the adsorbent (S) which explains these three characteristics of the adsorption:

- The surface of the adsorbent is in physical contact with a solution containing an adsorbate, strongly attracted to the surface.
- The surface has a specific number of sites where the adsorbate molecules can be adsorbed.
- The adsorption involves the attachment of only one layer of molecules or atoms to the surface, i.e., monolayer adsorption.

## 2.4 Literature Reviews

Indigo carmine (IC) is the most common chemical dye used as a model dye for the study of decomposition of organic dye. The presence of this dye causes the color change of water to deep blue even in very low concentration [45]. Many researchers reported the Indigo carmine degradation by using  $\text{TiO}_2$  as photocatalyst. Various treatments such as UV radiation, ozonation, sonolysis and combined methods were performed [46]. The maximum photodegradation of Indigo carmine was reported up to 100% when the combination of ozonation and sonolysis were used. Other organic dyes were also used as model dyes and studied. These dyes included methyl orange, methylene blue, reactive black 5 and reactive red 239. The summary of some studies were presented in Table 2.1.

**Table 2.1** the comparison of dye degradation with various methods by using  $\text{TiO}_2$  photocatalyst.

Materials	Methods	Organic dyes	%max Removal	Time	Ref
$\text{TiO}_2$	Ozonation/Sonolysis	Indigo Carmine	100%	6 min	[46]
$\text{TiO}_2$	Photocatalysis	Reactive Black 5	97%	120 min	
		Reactive Red 239	96%	120 min	[47]
$\text{TiO}_2$ / Chitosan	Photocatalysis	Methyl Orange	100%	360 min	
		Alizarin Red	100%	360 min	[18]
NP- $\text{TiO}_2$	Photocatalysis	Methyl Orange	69%	120 min	
		Methylene Blue	73%	120 min	[48]
NP- $\text{TiO}_2$	Photocatalysis	Methylene Blue	91%	420 min	
		Congo Red	90%	570 min	[49]

For the removal of heavy metal ions, many systems had been investigated. Various parameters had been studied including type of heavy metal ions and type of absorbents. Some selected data were in Table 2.3.

**Table 2.2** The comparison of heavy metal adsorption with various adsorbents

Adsorbent	Heavy metals	Maximum Adsorption Capacity	Ref
Chitosan	Cu(II)	1.76 mmol/g	
	Ni(II)	1.03 mmol/g	
	Zn(II)	1.3 mmol/g	[52]
	Pb(II)	13.05 mg/g	[40]
	Cd(II)	105 mg/g	[53]
	Cr(VI)	35.6 mg/g	[56]
Chitosan beads	Cr(III)	30.03 mg/g	
	Cr(VI)	76.92 mg/g	[54]
Chitosan/	Cu(II)	35.46 mg/g	
Epichlorohydrin	Zn(II)	10.21 mg/g	
	Pb(II)	34.13 mg/g	[40]
Chitosan/	Cu(II)	130.72 mg/g	
Epichlorohydrin/ triphosphate	Cd(II)	83.75 mg/g	
	Pb(II)	166.94 mg/g	[53]
Aminated- MCM-41	Cu(II)	1.52 mmol/g	
	Ni(II)	0.8 mmol/g	
	Zn(II)	0.83 mmol/g	[52]
Purolite CT-275	Cr(VI)	89.29 mg/g	
Purolite MN-500	Cr(VI)	126.58 mg/g	[55]
SWNTs	Cr(VI)	20.3 mg/g	
MWNTs	Cr(VI)	2.48 mg/g	[56]

## CHAPTER 3

### RESEARCH METHODOLOGY

#### 3.1 Materials

##### 3.1.1 Chemicals

Chromium (VI) oxide

Copper (II) sulphate

Ethanol

Epichlorohydrin

Glutaraldehyde

Indigo carmine

Long chain chitosan (90% deacetylation)

Sodium hydroxide

Standard Cr (VI) solution 1000 ppm

Titanium dioxide (Rutile)

##### 3.1.2 Equipment

Inductively coupled plasma - atomic emission spectroscopy

Optical microscope

pH meter

UV/Vis spectrophotometer

### 3.2 Preparation of TiO<sub>2</sub>/Chitosan microbeads with crosslinking agents

The 2 wt% chitosan was added to 0.5 wt% acetic acid then it was stirred magnetically for 6 hours to obtain homogeneous chitosan solution. Various amounts of added TiO<sub>2</sub> powder were studied i.e. 1, 3 and 5 wt%. Each TiO<sub>2</sub> batch was added to chitosan solution and mixed well. The TiO<sub>2</sub>/Chitosan mixture was loaded into a syringe with various needle size i.e., 16 and 20 gauge and injected dropwise into 3 M NaOH dissolved in 1:2 volume ratio of ethanol:water mixture solvent to obtain TiO<sub>2</sub>/Chitosan microbeads. Finally, the obtained beads was soaked into 0.1 M epichlorohydrin or glutaraldehyde and kept for a given time for the crosslinking process.

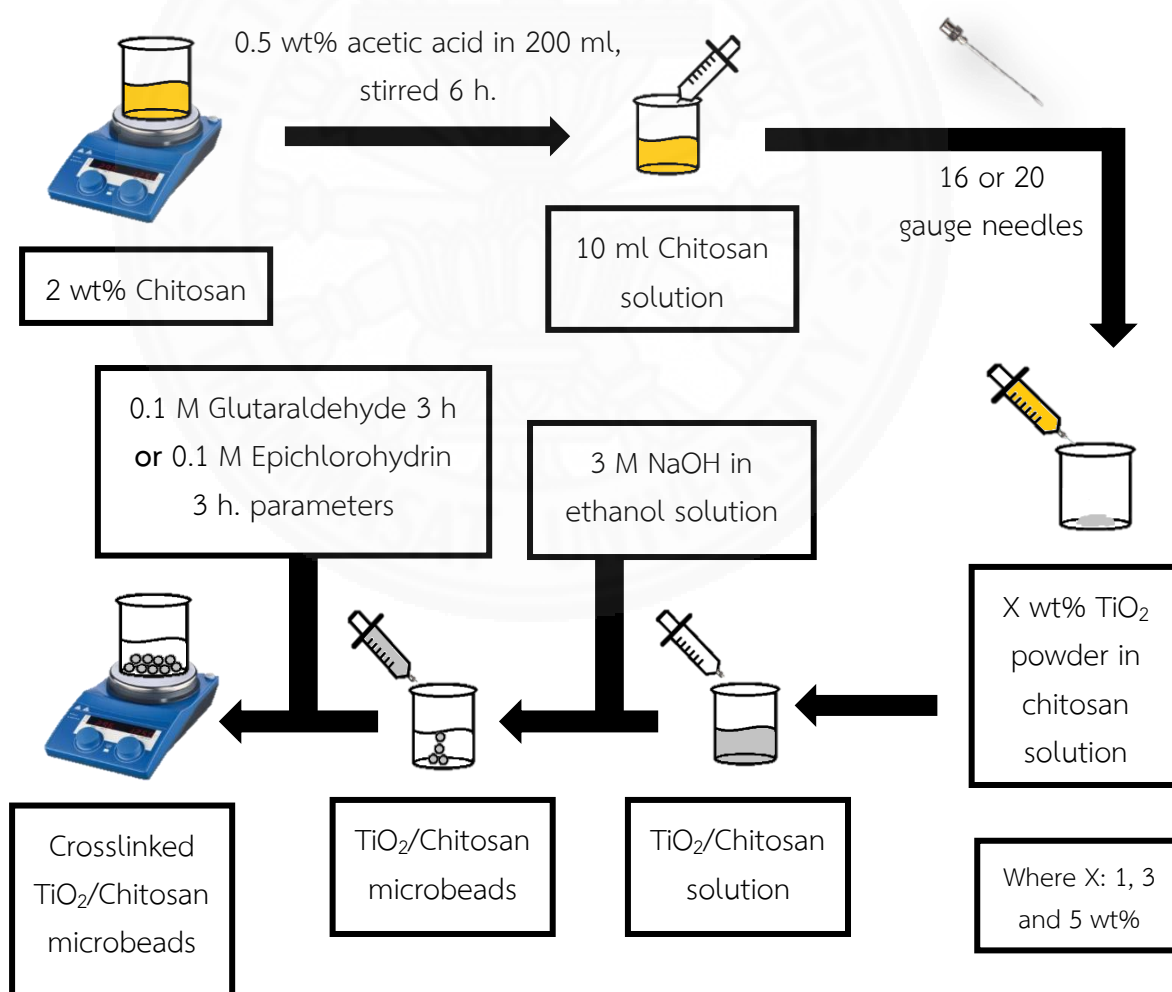
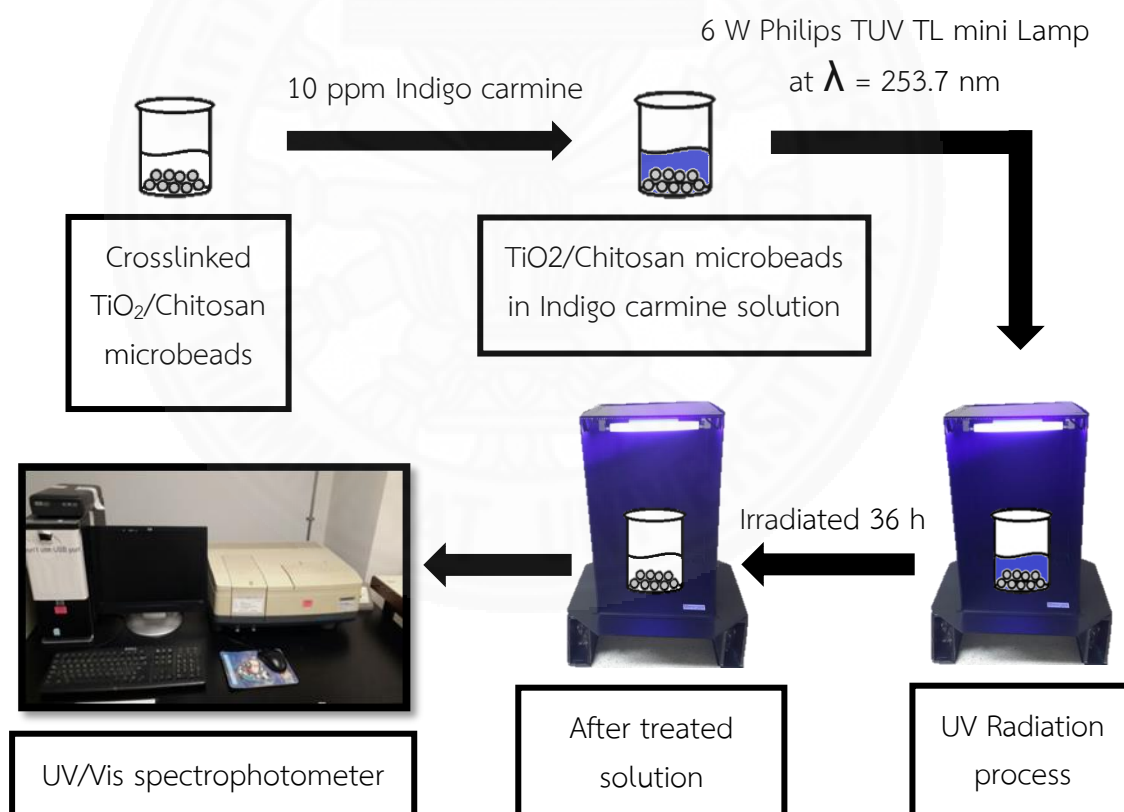


Figure 3.1 The preparation of TiO<sub>2</sub>/Chitosan microbeads.

### 3.3 Dye decomposition experiment and analysis

The 10 ppm Indigo carmine stock solution was prepared by dissolving 1 g of indigo carmine disodium disulfonate salt in 1 liter of deionized water. From this stock solution, 10 ppm dye solution was prepared. The fixed amount of TiO<sub>2</sub>/Chitosan microbeads was soaked into 10 ppm dye solution. The obtained mixture was stirred magnetically and irradiated by Philips TL 6W actinic BL UV lamp for 36 hrs. The solution was sampled to determine the concentration of Indigo carmine via UV-Visible Spectrophotometer. The concentration of Indigo carmine was changed to 100 ppm for the study of the multifunctional properties of TiO<sub>2</sub>/Chitosan microbeads with presence of Cr (VI) ions and was determined by above mentioned method for the concentration of the remaining Indigo carmine.



**Figure 3.2** The Dye decomposition experiment.



The concentration of remaining dye is the measure of quantity presented in the solution. This amount of dye was measured through UV-Vis spectrophotometer. The dye degradation is presented by a first order equation as

$$C_t = C_0 e^{-kt} \quad (3.1)$$

The percentage of dye degradation was calculated by,

$$\% \text{ Degradation} = \left[ 1 - \frac{C_t}{C_0} \right] \times 100 \quad (3.2)$$

Where  $C_0$  is concentrations of dye in the solution before UV-exposure and  $C_t$  is concentrations of dye in the solution after UV-exposure,  $t$  is the time duration of exposure, and  $k$  is degradation reaction rate constant.  $C_0$  and  $C_t$  are directly proportional to the intensity of absorption peak of dye.

### 3.4 Heavy metal adsorption experiment and analysis

The 1000 ppm Cr (VI) stock solution was prepared by dissolving  $\text{CrO}_3$  in deionized water and used as a model metal ion contaminant. The fixed amount of  $\text{TiO}_2$  / Chitosan microbeads was added to 100 ml of heavy metal solution. The concentration of Cr (VI) was measured periodically via inductively coupled plasma – optical emission spectrometry or ICP-OES.

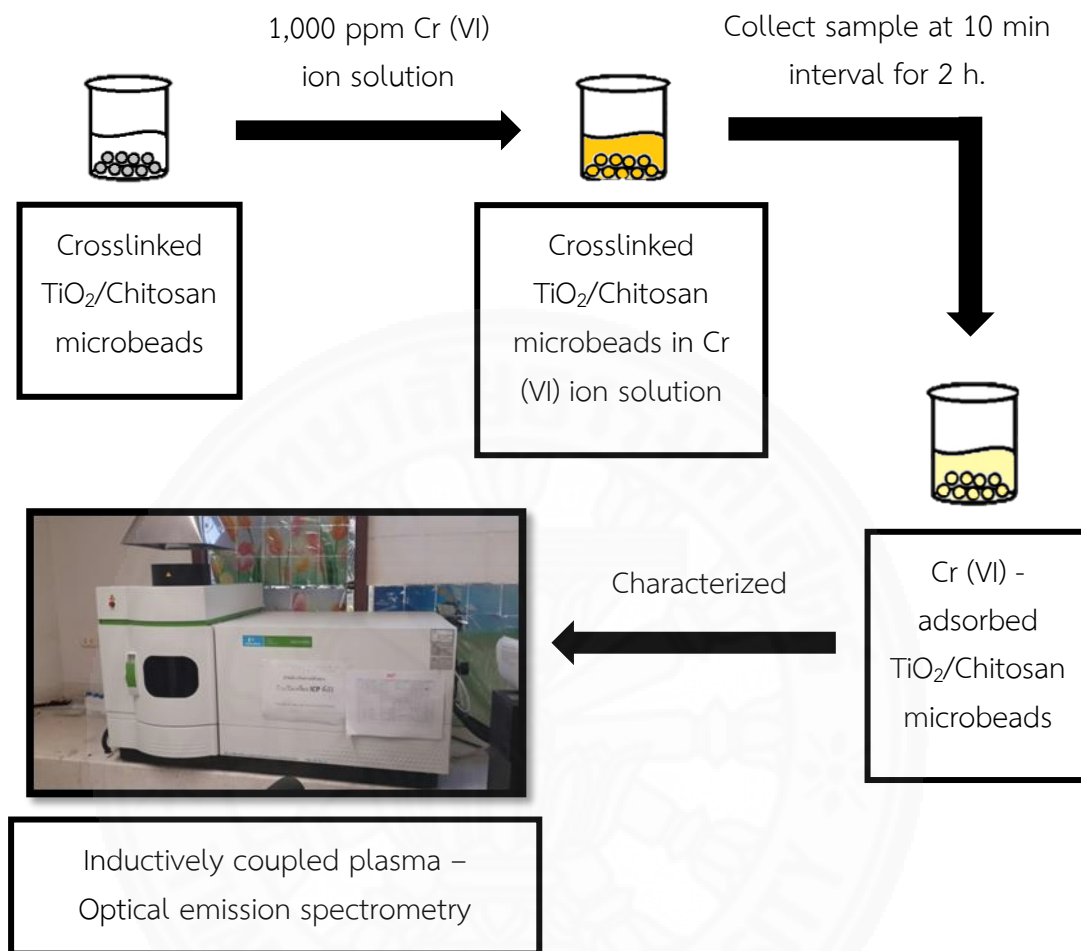


**Figure 3.3** The heavy metal adsorption experiment.

In addition, the adsorption isotherm can be calculated using Langmuir isotherm. The Langmuir equation is given as

$$q_{eq} = \frac{Q^0 b C_{eq}}{1 + b C_{eq}} \quad (3.3)$$

Where  $Q^0$  is the maximum amount of the metal ion per unit weight of microbeads to form a complete monolayer on the surface bound at high  $C_{eq}$  ( $\text{mg}\cdot\text{g}^{-1}$ ) and  $b$  is a constant related to the affinity of the binding sites,  $Q^0$  represents a

practical limiting adsorption capacity when the surface is fully covered with metal ions and assists in the comparison of adsorption performance, particularly in cases where the sorbents did not reach its full saturation in experiments.  $Q$  and  $b$  can be determined from the linear plot of  $1/q_{eq}$  vs.  $C_{eq}$ .

Heavy metal adsorption capacity and percentage of metal ion removal performance were calculated by equations as follow:

$$\text{Adsorption capacity, } q \text{ (mg}\cdot\text{g}^{-1}\text{)} = \frac{C_0 - C_t}{m} V \quad (3.4)$$

$$\text{Removal performance (\%)} = \frac{C_0 - C_t}{C_0} \cdot 100 \quad (3.5)$$

Where  $C_0$  and  $C_t$  are initial and final concentrations of Cr (VI) ( $\text{mg}\cdot\text{L}^{-1}$ ),  $m$  is the mass of adsorbent (g) and  $V$  is volume of heavy metal ion solution (mL).

### 3.5 Multifunctional properties experiment and analysis

The mixture of 1000 ppm Cr (VI) and 100 ppm indigo carmine was prepared by dissolving 1 g of  $\text{CrO}_3$  in 1 L of deionized water, to get homogeneous solution then adding 0.1 g Indigo carmine into 1000 ppm Cr (VI) solution. For each experiment, 100 mL of obtained solution was used. The concentrations of Indigo carmine and Cr (VI) were determined by UV-Vis spectroscopy and ICP-OES, respectively. The results will showed the influence of dye degradation and metal adsorption of  $\text{TiO}_2$ /Chitosan microbeads. The multifunction property experiment was presented in figure 3.4.

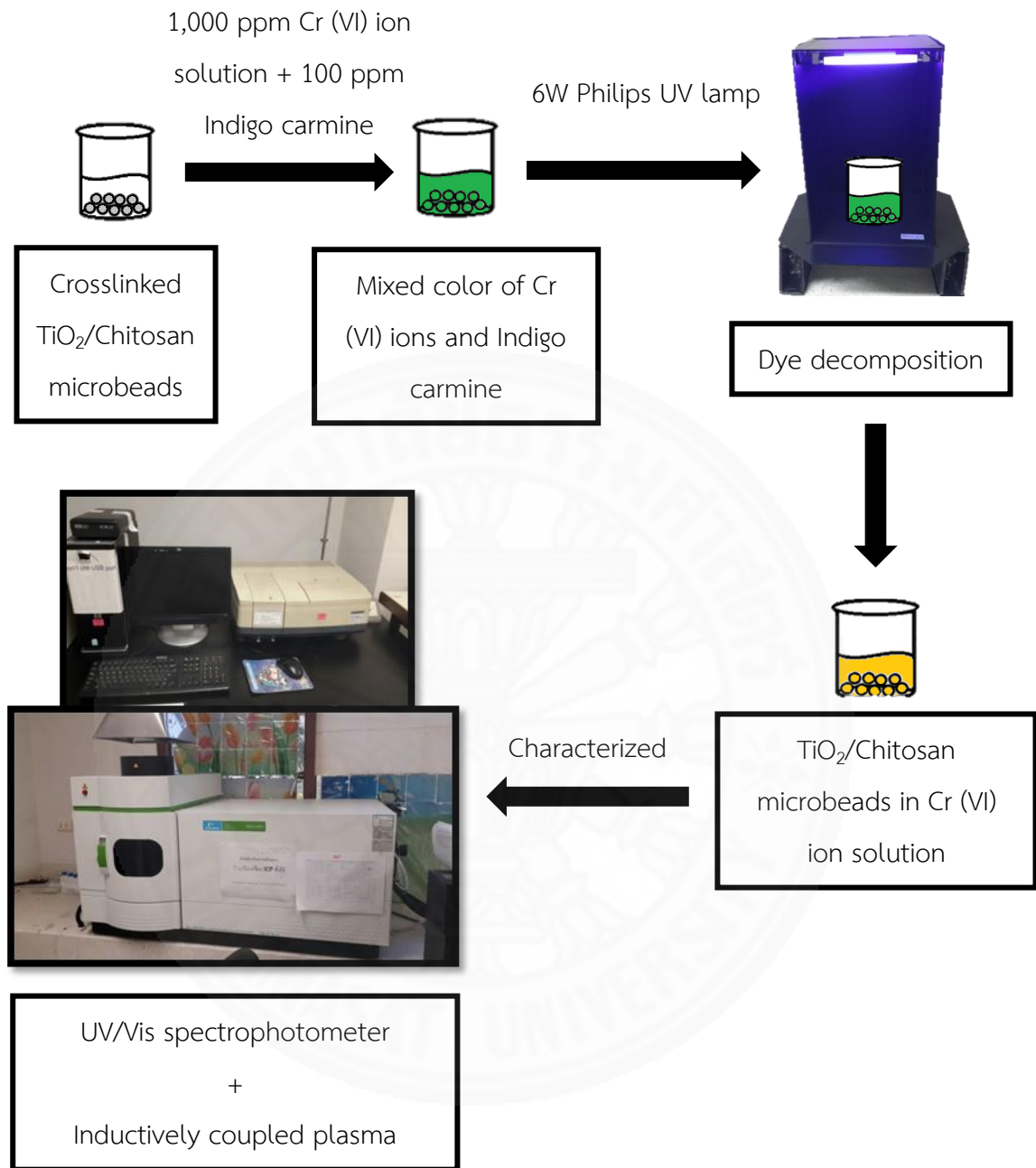
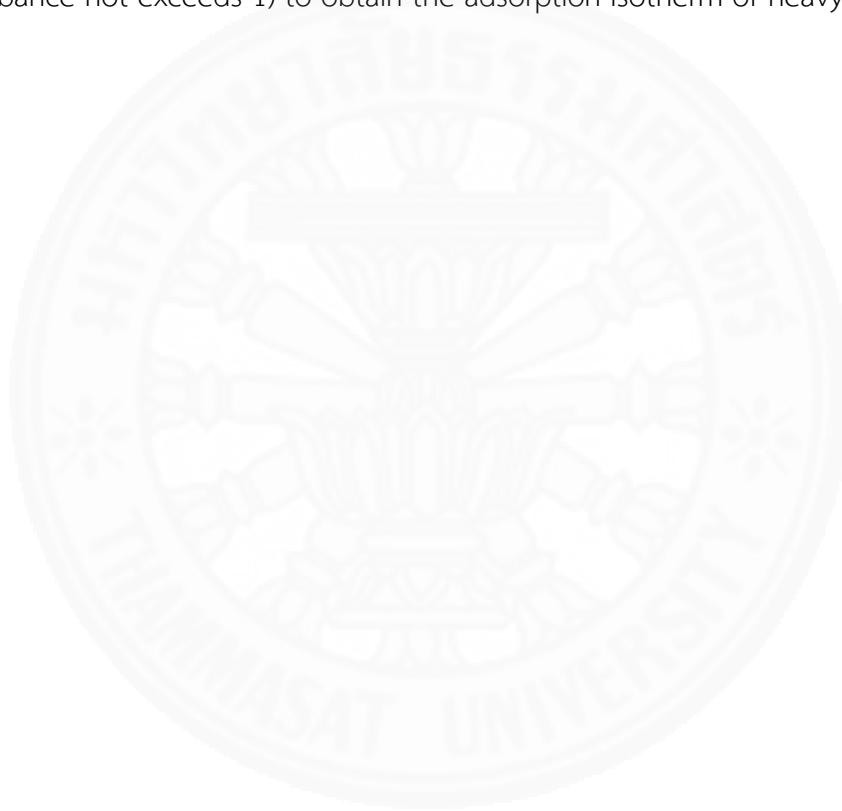


**Figure 3.4** The study of multifunctional properties.

Multifunctional properties were analyzed by using both UV/Vis spectrophotometer and ICP-OES. The samples were divided into 2 parts and analyzed separately to acquired data. For UV/Vis spectrophotometer, samples' concentration were diluted by 10 times (decreased the concentration from 100 ppm to 10 ppm so that the absorbance not exceeds 1) to obtain the percentage of photodegradation. For ICP-OES technique, samples' concentration were diluted by 40 times (decreased the concentration from 1000 ppm to 25 ppm so that the absorbance not exceeds 1) to obtain the adsorption isotherm of heavy metal ions.



## CHAPTER 4

### RESULTS AND DISCUSSION

#### 4.1 The photodegradation of TiO<sub>2</sub> rutile powder

The results of TiO<sub>2</sub> rutile powder were shown in figure 4.1. Experiment condition was set as 0.3 g of TiO<sub>2</sub> powder was added into 10 ppm Indigo carmine solution and exposed to UV radiation using a Philips TL 6W actinic BL UV lamp to obtain the data and compared to TiO<sub>2</sub>/chitosan composite. The result showed that with the powder form of TiO<sub>2</sub>, the photodegradation process was successfully decomposed up to 98.72% of Indigo carmine in 12 hours as shown in Figure 4.1.

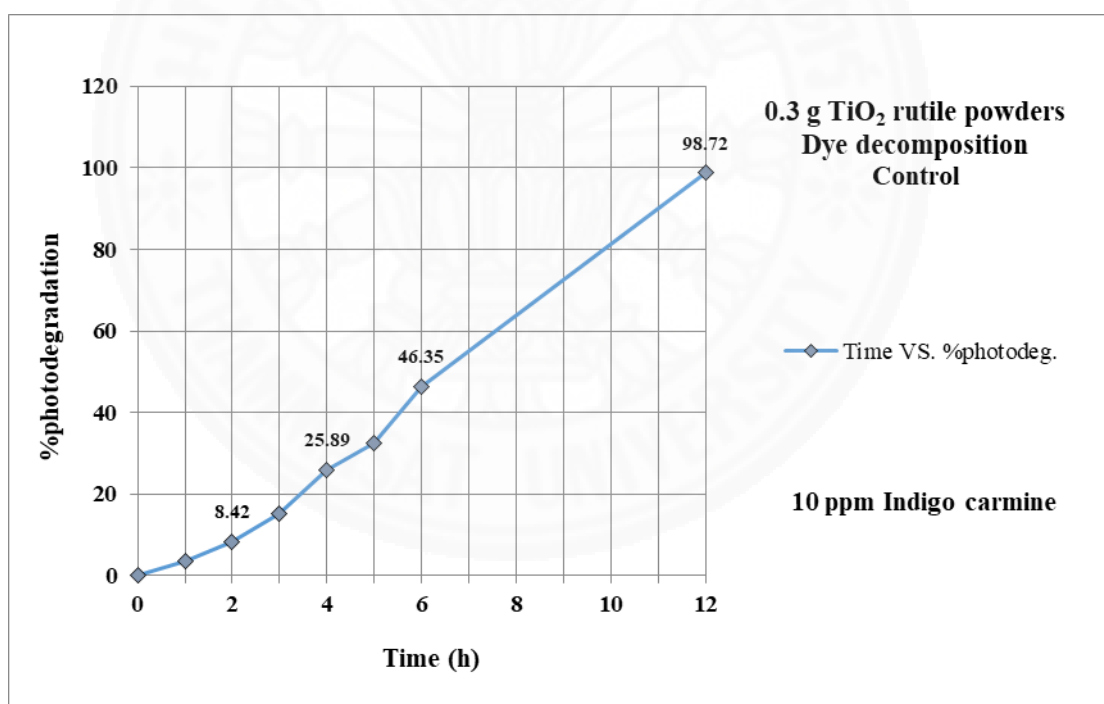


**Figure 4.1** The percentage of photodegradation of 10 ppm Indigo carmine solution using 0.3 g of TiO<sub>2</sub> powder.

## 4.2 The photodegradation of Indigo carmine with TiO<sub>2</sub>/Chitosan microbeads

### 4.2.1 Effect of the amount of TiO<sub>2</sub> microbeads on the photodegradation of Indigo carmine

In this study, the amounts of 3 wt% TiO<sub>2</sub>/Chitosan microbeads were varied i.e., 1 and 2 g to compare their photocatalytic effect. The results showed that the decomposition of Indigo carmine depended on the amount of TiO<sub>2</sub>/Chitosan microbeads used as shown in Figure 4.2. The more the amount of TiO<sub>2</sub>/Chitosan microbeads used, the higher the decomposition of Indigo carmine. With using 2 g of TiO<sub>2</sub>/Chitosan microbeads, the decomposition of Indigo carmine could be up to 85.91% within 36 hours. The results suggested that the decomposition of Indigo carmine could be speeded up when more composites were added.

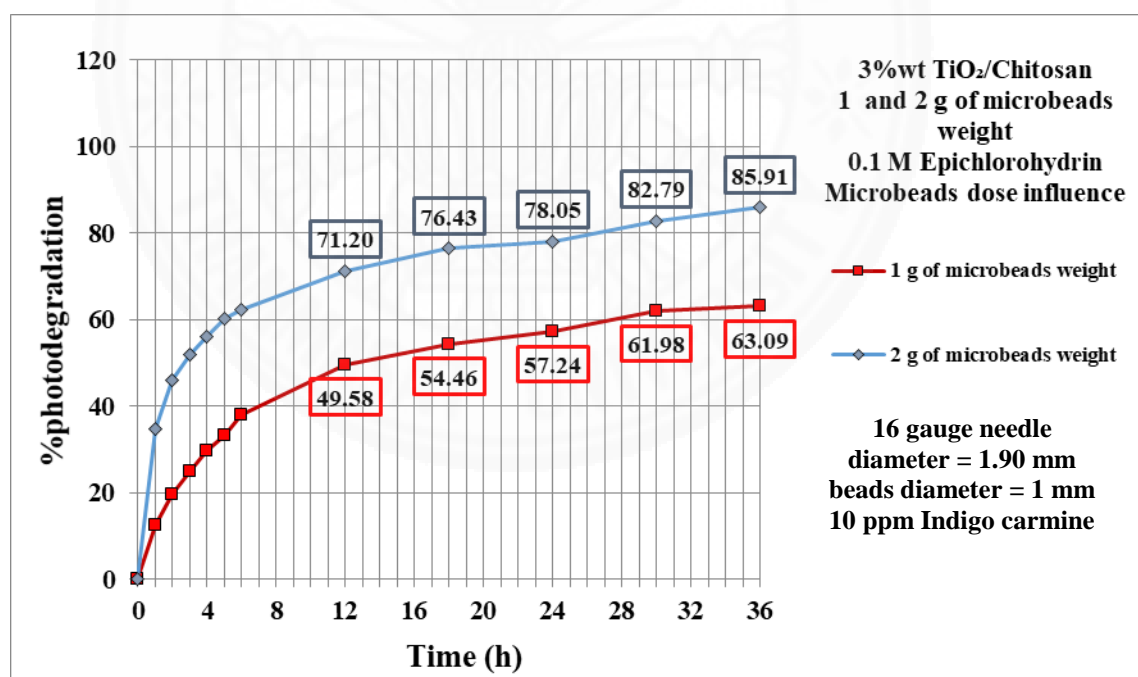


Figure 4.2 The effect of the amount of beads used on the decomposition of dye.

#### 4.2.2 Effect of crosslinking agents used to strengthen the microbeads on the photodegradation of Indigo carmine

Two sets of TiO<sub>2</sub>/Chitosan microbeads using different crosslinking agents, i.e., glutaraldehyde and epichlorohydrin were prepared for this study. The preparation process was mentioned earlier. In brief, fixed amount of TiO<sub>2</sub> powder was added into 2 wt% chitosan solution and then injected to form microbeads using syringe with 16 gauge needle size into 3M NaOH solution. All of the obtained microbeads were then filtered and soaked into crosslinking agent solutions. The solutions of 0.1M glutaraldehyde and epichlorohydrin crosslinking agents were used. This process was needed to strengthen the microbeads, so that they could be used multiple times without breaking apart.

The results as shown in Figure 4.3 and 4.4 revealed that microbeads with glutaraldehyde as a crosslinking agent gave better performance compared to those with epichlorohydrin. The decomposition of Indigo carmine was up to almost 100% within shorter time i.e., 24 hours compared to more than 36 hours, when glutaraldehyde was used as a crosslinking agent.

As mentioned earlier, these two crosslinking agents link chains of chitosan molecules at different functional groups. Glutaraldehyde links at amine groups while epichlorohydrin links at hydroxyl groups. This means there will be less crosslinking points for glutaraldehyde because of less numbers of amine groups compared to hydroxyl groups. The experimental results suggested that it might due to the physical feature of microbeads that more loosen up or in other words, they were lighter cross-linked when 0.1M glutaraldehyde was used. Therefore the dye molecules could penetrate into the beads and interact with more TiO<sub>2</sub> particles embedded inside.

Although, the photodegradation performance of microbeads cross-linked with glutaraldehyde was better, their stability in acidic solution was worse than those beads cross-linked with epichlorohydrin. The TiO<sub>2</sub>/chitosan microbeads cross-linked with glutaraldehyde couldn't be reused since some of them were crumbled after the first use. Therefore, the rest of the experiments, the



epichlorohydrin was chosen to be used as the crosslinking agent, since multiple uses were required as one of the expected outcomes of the study.

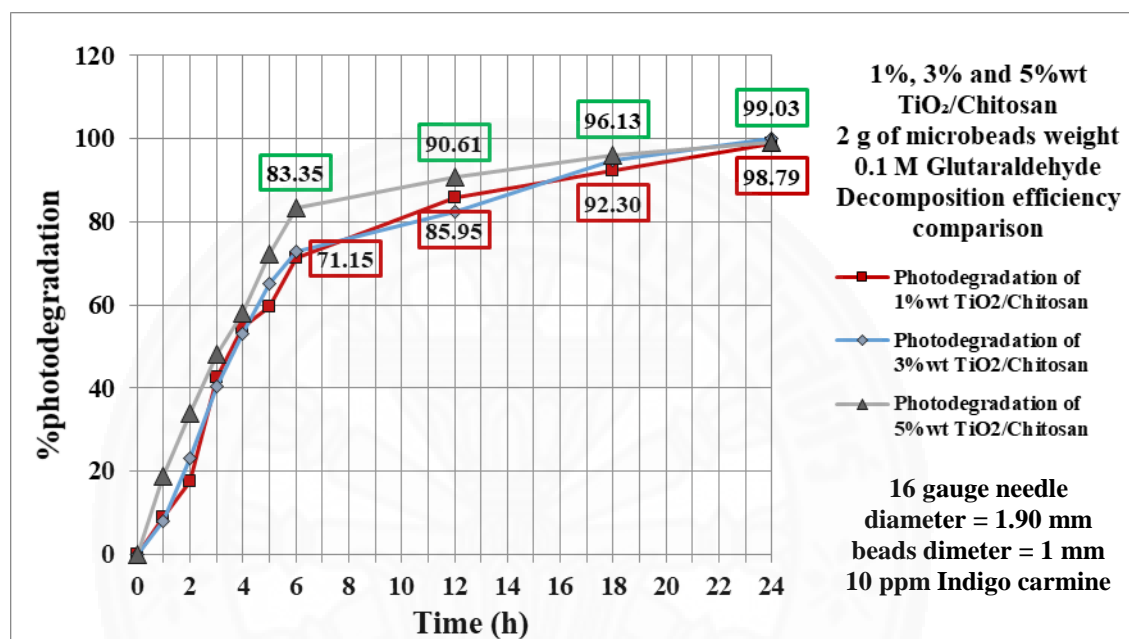


**Figure 4.3** The photodegradation of dye with 2 g of 1, 3 and 5 wt% of TiO<sub>2</sub> embedded into chitosan microbeads cross-linked with glutaraldehyde.

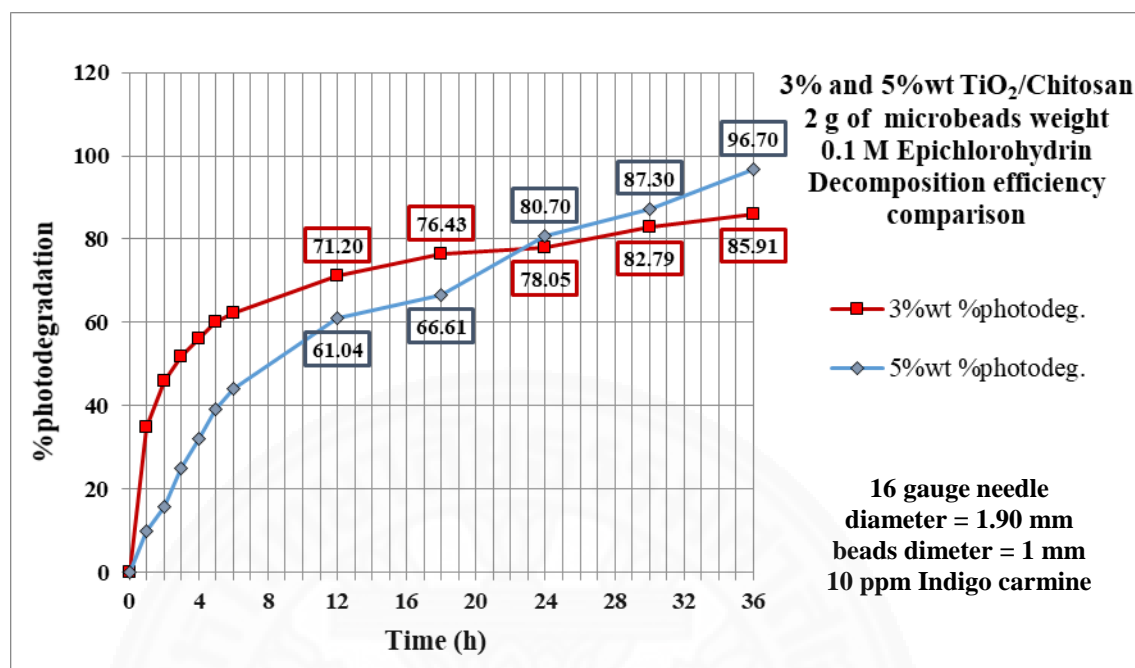


**Figure 4.4** The photodegradation of dye with 2 g of 3 and 5 wt% of TiO<sub>2</sub> embedded into chitosan microbeads and cross-linked with epichlorohydrin (ECH).

#### 4.2.3 The study of recyclability of the TiO<sub>2</sub>/chitosan microbeads

In this study, two parameters i.e., crosslinking agent's concentration and needle size were varied. The solutions of epichlorohydrin with the concentrations of 0.1 and 0.5 M were prepared and used in the crosslinking process. The TiO<sub>2</sub>/chitosan microbeads were fabricated using 2 needle sizes i.e., 16 and 20 gauge sizes. The actual outside diameter of these needles are 1.90 and 0.9 mm., respectively. The obtained microbeads had the average diameter of 1.0 and 0.5 mm., when 16 and 20 gauge needle were used, respectively. The amount of microbeads was fixed at 2 g. The amount of loaded TiO<sub>2</sub> was fixed as well at 3 wt%.

As shown in Figure 4.5 and 4.6, the higher the concentration of crosslinking agent used, the lower the decomposition of Indigo carmine. This result can simply explained on the fact that the higher the concentration of crosslinking agent, the tighter the microbeads. As a result, less numbers of Indigo carmine

molecules would be able to penetrate into the beads where more  $\text{TiO}_2$  particles were present leading to less interaction with  $\text{TiO}_2$ .

For the ability of  $\text{TiO}_2$ /chitosan microbeads to be reused, it was found that the prepared composites i.e., 3 wt% loaded  $\text{TiO}_2$  with epichlorohydrin as the crosslinking agent, survived up to the fourth recycle time. After that, most of the microbeads got crumbled before the photodegradation was completed. Moreover, the significant reduction in degradation performance was noticed after the second recycle as shown in Figure 4.5, 4.6 and 4.7.

When the needle size was altered, it was found that the smaller the diameter of the needle, the smaller the diameter of the microbeads leading to the faster the photodegradation of Indigo carmine within the given time as shown in Figure 4.5 and 4.7. This was probably due to more surface areas of the smaller beads creating more contacting points between  $\text{TiO}_2$  particles and Indigo carmine molecules. However, the differences were insignificant. The percentages of Indigo carmine decomposed within the given time were in the same magnitude and could be considered as the same.

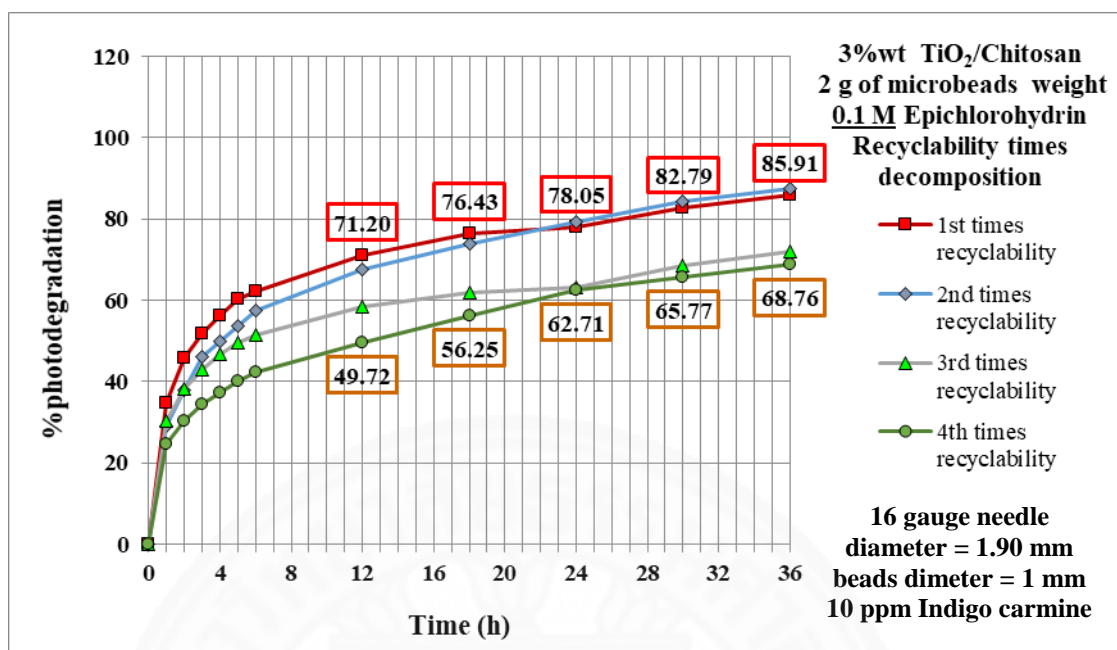


Figure 4.5 The recyclability of 2 g of 3wt% TiO<sub>2</sub>/Chitosan microbeads cross-linked with 0.1 M epichlorohydrin and ran by 16 gauge needle size.

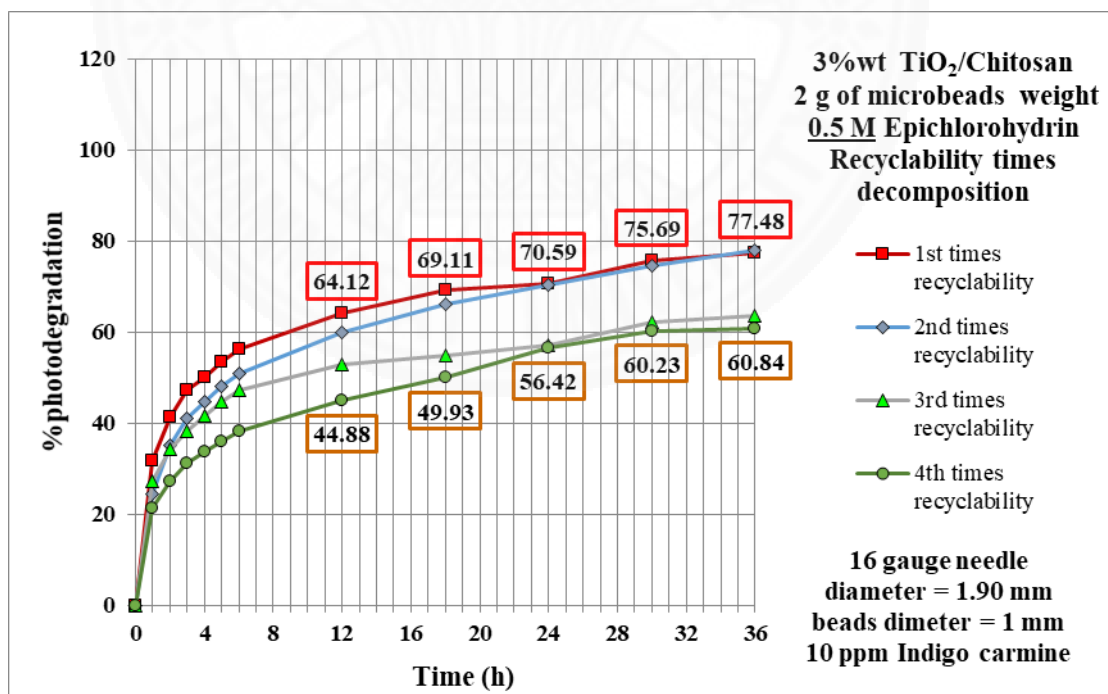
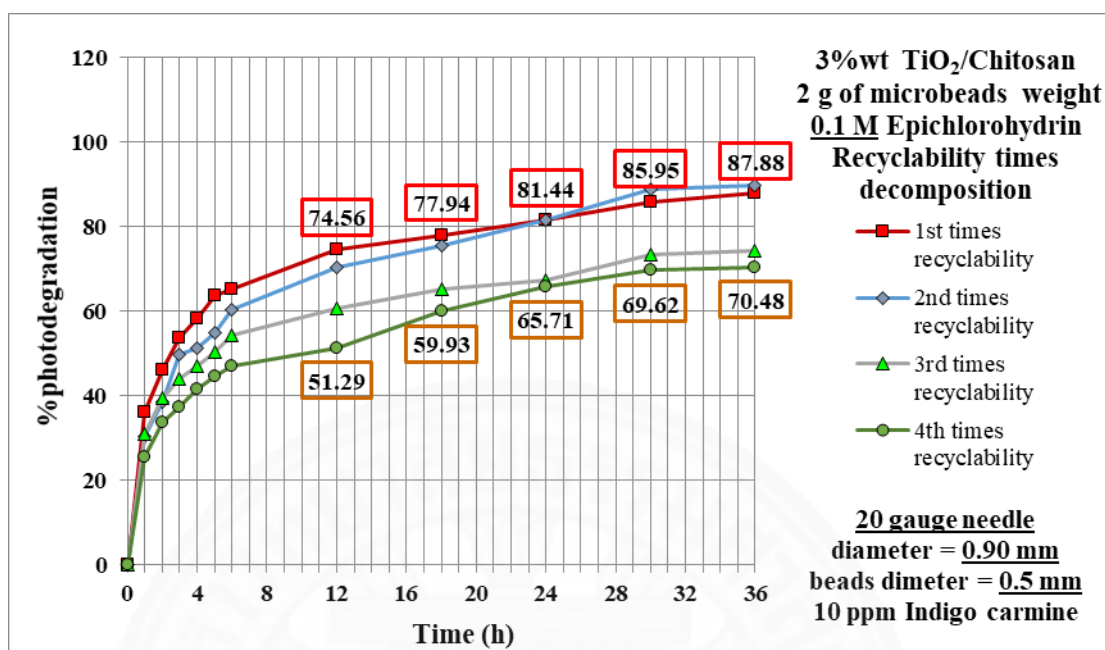


Figure 4.6 The recyclability of 2 g of 3wt% TiO<sub>2</sub>/Chitosan microbeads cross-linked with 0.5 M epichlorohydrin and ran by 16 gauge needle size.



**Figure 4.7** The recyclability of 2 g of 3wt% TiO<sub>2</sub>/Chitosan microbeads cross-linked with 0.1 M epichlorohydrin and ran by 20 gauge needle size.

#### 4.2.4 The optical microscope image of microbeads with various crosslinking agents

Microbeads images were captured by optical microscope with 40 x magnifiers to observe the distribution of TiO<sub>2</sub> powder embedded into chitosan beads, and to measure the average size of microbeads. Images were shown in Figure 4.8 and 4.9. The color difference of these two images was probably due to the aging of glutaraldehyde used in this preparation. It was believed that this was nothing to do with its property as a crosslinking agent.

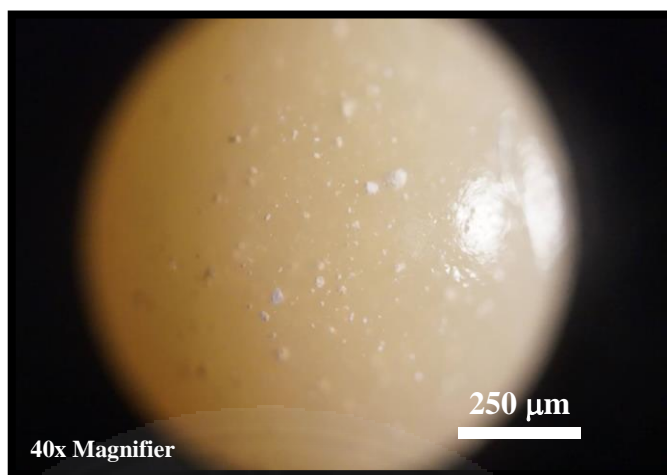


**Figure 4.8** The microscopic image of 3 wt% TiO<sub>2</sub>/Chitosan cross-linked with Glutaraldehyde crosslinking agent.

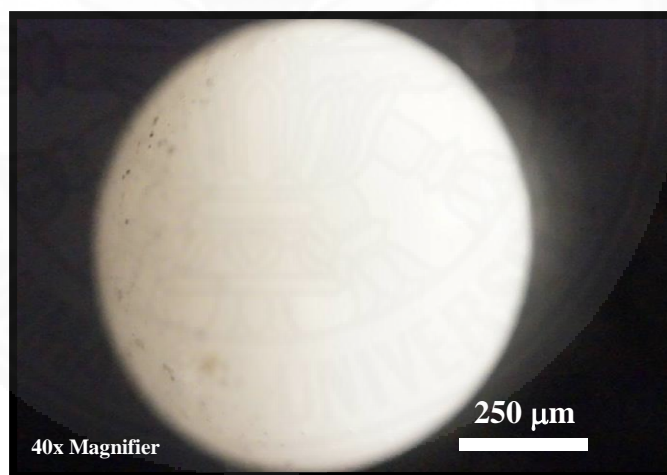


**Figure 4.9** The microscopic image of 3 wt% TiO<sub>2</sub>/Chitosan cross-linked with Epichlorohydrin crosslinking agent.

### 4.3 The Cr (VI) adsorption isotherm of TiO<sub>2</sub>/Chitosan microbeads

The Cr (VI) ion adsorption isotherm of TiO<sub>2</sub>/Chitosan microbeads was measured by using data collected from ICP-OES technique. The studies were performed in two conditions i.e., with and without the presence of Indigo carmine. This kinetic study was carried out with using 2 g of 3 wt% TiO<sub>2</sub>-loaded Chitosan microbeads cross-linked with 0.1 M epichlorohydrin as the crosslinking agent. The concentration of Cr (VI) ions was started at 1000 mg/L and its original pH of 5. The absorption of Cr (VI) was determined until the equilibrium was reached so that all required parameters could be determined as needed for the study of adsorption isotherm as shown in Table 4.1.

**Table 4.1** Kinetic parameters of Cr (VI) adsorption for Langmuir isotherm with and without the presence of Indigo carmine.

Kinetic parameters	With Indigo carmine	Without Indigo carmine
$q_{\max}$ (mg·g <sup>-1</sup> )	28.25	31.45
$K_l$ (min <sup>-1</sup> )	0.017	0.023
$R^2$	0.9991	0.9998

The maximum adsorption capacity ( $q_{\max}$ ) was slightly lower than that from Chanil Jung's study [56], which was found to be 35.6 mg/g of chitosan. This was probably due to the presence of TiO<sub>2</sub> particles that tightly stuck on chitosan microbeads and became obstacles to the chelation of Cr (VI) ions with chitosan's amine functional groups.

As shown in Table 4.1, the kinetic parameters of the adsorption of Cr (VI) by TiO<sub>2</sub>/chitosan microbeads with or without the presence of Indigo carmine were insignificantly different. This implies that the kinetic of the adsorption of Cr (VI) ions by chitosan microbeads is not altered by the presence of Indigo carmine.

Moreover, the kinetic parameters calculated to fit with the Langmuir isotherm (a better fitted, compared to Frundrich isotherm) were also in consistent no matter with or without Indigo carmine, as shown in Figure 4.12.

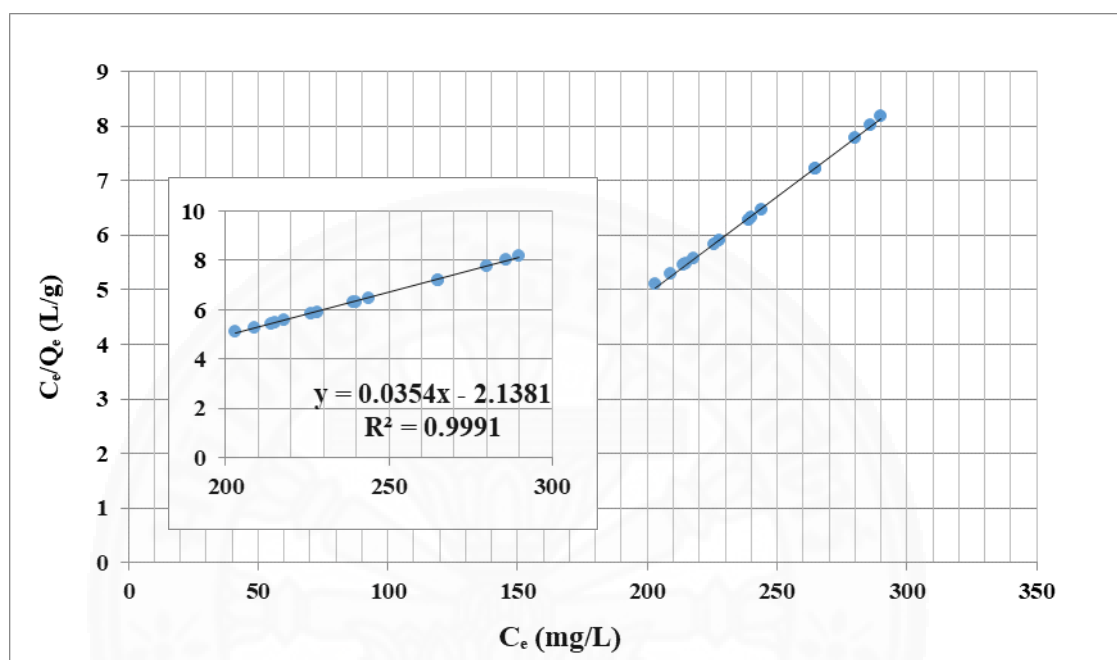


**Figure 4.10** Langmuir isotherms of Cr (VI) ions with  $\text{TiO}_2$ /Chitosan microbeads without the presence of Indigo carmine.

As known by the term Langmuir isotherm, the adsorption of Cr (VI) by these  $\text{TiO}_2$ /chitosan microbeads was occurred with a single layer of molecules (or atoms) attached on the surface of microbeads. However, due to the porosity of microbeads, it was believed that Cr (VI) ions could get inside the beads and attached to amine groups due to the electrostatic interactions. So, the adsorption did not occur only on the outer surface of the microbeads but also to the chitosan molecules inside.



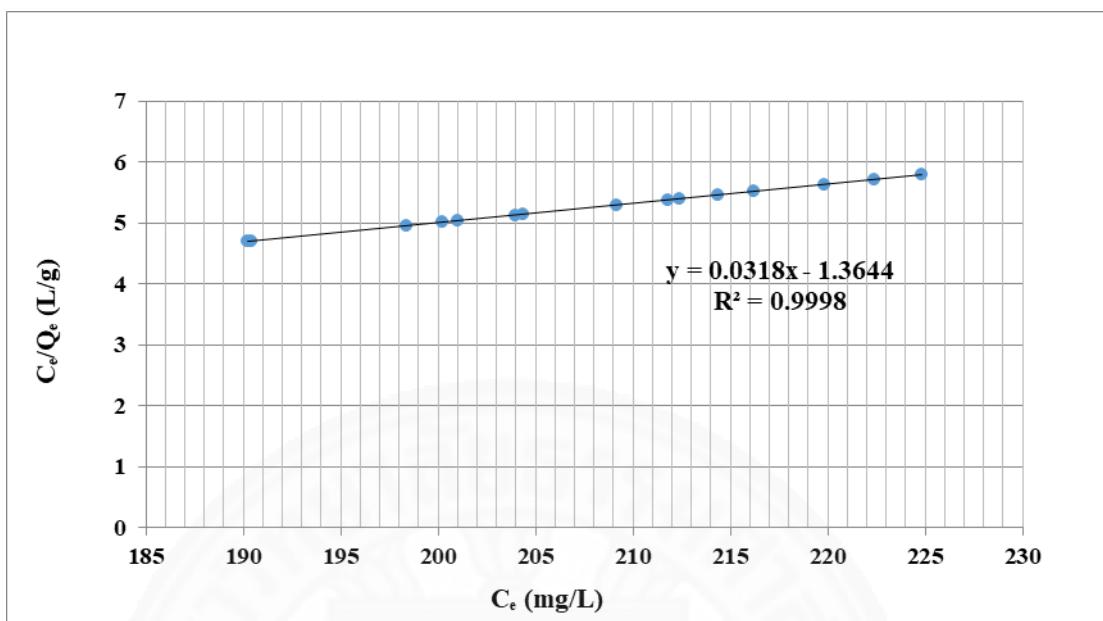


Figure 4.11 Langmuir isotherms of Cr (VI) ions with  $TiO_2$ /Chitosan microbeads with the presence of Indigo carmine.

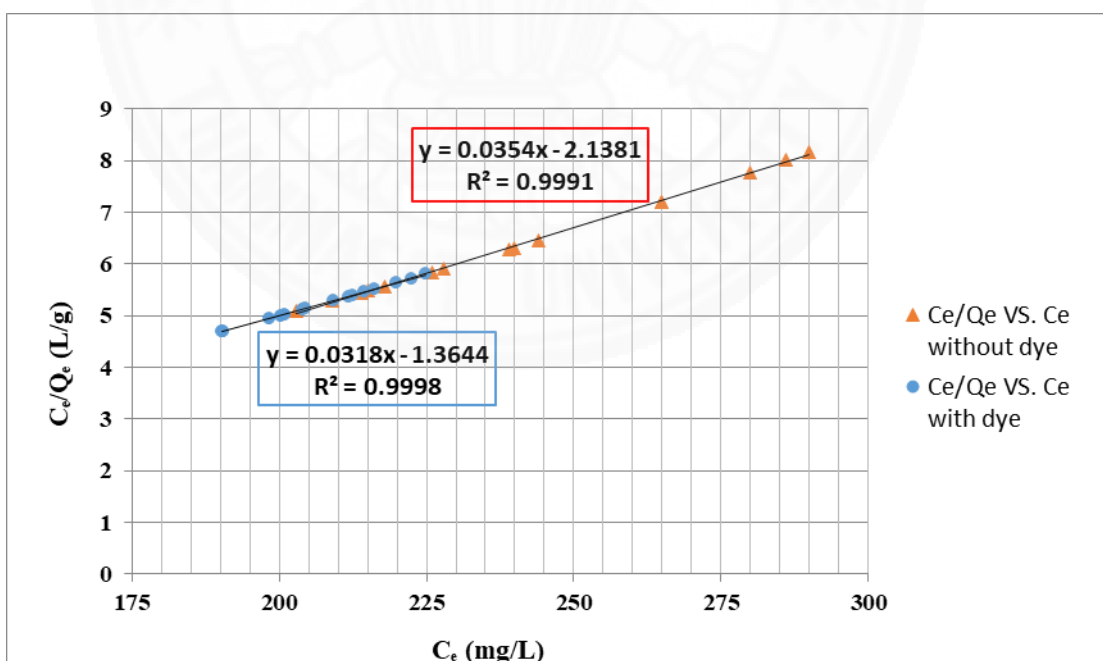


Figure 4.12 Langmuir isotherms of Cr (VI) ions with  $TiO_2$ /Chitosan microbeads with and without the presence of Indigo carmine on the same plot.

#### 4.4 Multifunctional properties of TiO<sub>2</sub>/Chitosan microbeads

Two properties of prepared TiO<sub>2</sub>/chitosan microbeads were investigated simultaneously namely as the bio-adsorbent and photocatalyst. The 2 g of 3 wt% TiO<sub>2</sub>/chitosan microbeads cross-linked with 0.1 M epichlorohydrin solution was used. The solution containing 1000 mg/L of Cr (VI) ions and 100 mg/L of Indigo carmine was used.

As shown in Figure 4.13, it was found that within one hour, the decomposition of Indigo carmine was over 90%, which was a lot faster compared to previous conditions. Within 4 hours, Indigo carmine had degraded to almost 100%. For the adsorption of Cr (VI) ions, the concentration of Cr (VI) ions went down to its equilibrium at 80% adsorbed within one hour.

It turned out that the decomposition of Indigo carmine somehow happened with the rate three times faster than that of condition without the presence of Cr (VI) ions. It might be due to the interaction of TiO<sub>2</sub> with Cr (VI) ions before the adsorption leading to more hydroxyl radicals generated. These radicals are responsible for the decomposition of the Indigo carmine molecules. The effect of Cr (VI) ions on the decomposition of Indigo carmine was quite unique since there had been no other reports with other metal ions that showed similar results.

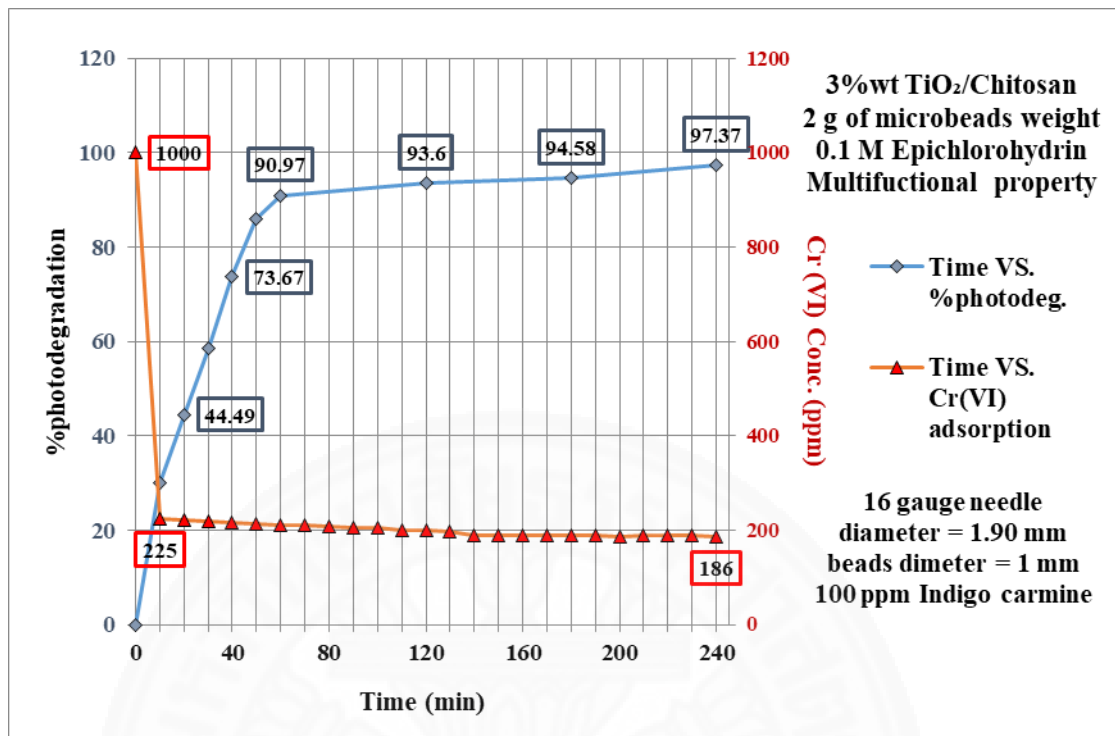


**Figure 4.13** The multifunctional properties of TiO<sub>2</sub>/Chitosan microbeads soaked into the solution containing of both Cr (VI) ions and Indigo carmine.

## CHAPTER 5

### CONCLUSIONS

The TiO<sub>2</sub>/Chitosan microbeads were successfully prepared. The concentration of chitosan was chosen to be 2 wt%, which made it easier for the microbeads to be formed. The maximum amount of loaded TiO<sub>2</sub> was 3 wt% in order to get better dispersion of particles in chitosan solution. The microbeads were cross-linked with either epichlorohydrin or glutaraldehyde for three hours.

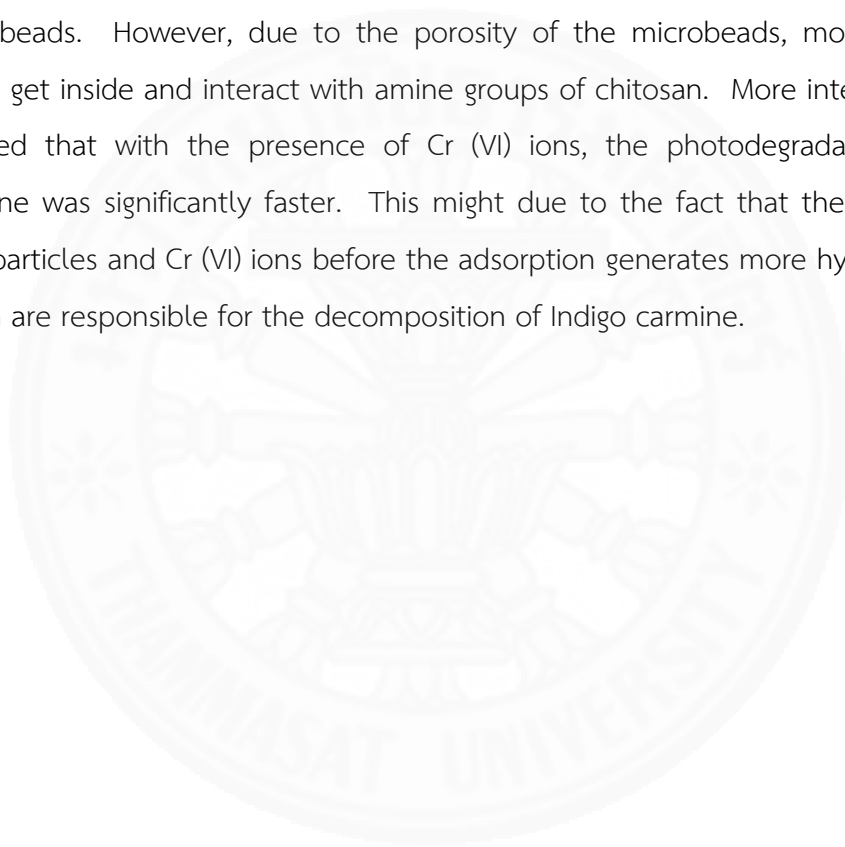
The decomposition of Indigo carmine with 2 g of TiO<sub>2</sub>/Chitosan microbeads under the exposure of UV-radiation reached almost 100% within 24 hours when 0.1M glutaraldehyde was used as the crosslinking agent compared to only 80% when 0.1M epichlorohydrin was used as the crosslinking agent. However, due to instability under acidic condition of microbeads cross-linked with glutaraldehyde, the epichlorohydrin was chosen to be the crosslinking agent for this research.

It was found that the more the amount of TiO<sub>2</sub>/Chitosan microbeads, the faster the decomposition of Indigo carmine. This was simply due to more TiO<sub>2</sub> particles, which were the active species for the decomposition of Indigo carmine when exposed to the UV radiation. Moreover, the smaller the size of the TiO<sub>2</sub>/Chitosan microbeads, the faster the decomposition of Indigo carmine. This could be explained in terms of more physical contact between TiO<sub>2</sub> and Indigo carmine molecules. However, with the scope of this research, the two different sizes microbeads showed insignificant results of the decomposition of Indigo carmine.

The recyclability of TiO<sub>2</sub>/Chitosan microbeads was investigated. It was found that with 0.1M epichlorohydrin as the crosslinking agent, the microbeads could be repeatedly used up to four times before getting crumbled. The reuse of microbeads was done without any treatment making them very suitable in actual applications. However, after the second use, the capability of these microbeads to decompose Indigo carmine decreased dramatically but still within acceptable values.

Other parameters are needed to be taken into consideration especially the amount of microbeads when recycling is a must.

The ability of TiO<sub>2</sub>/Chitosan microbeads to adsorb metal ions is due to the presence of the amine functional groups on chitosan chains. With the presence of Indigo carmine, the adsorption of Cr (VI) ions was intact. The adsorption of Cr (VI) ions by TiO<sub>2</sub>/Chitosan microbeads was fitted nicely with Langmuir isotherm indicating that only single layer of molecules (or atoms) was attached to the surface of microbeads. However, due to the porosity of the microbeads, more Cr (VI) ions could get inside and interact with amine groups of chitosan. More interesting results showed that with the presence of Cr (VI) ions, the photodegradation of Indigo carmine was significantly faster. This might be due to the fact that the interaction of TiO<sub>2</sub> particles and Cr (VI) ions before the adsorption generates more hydroxyl radicals which are responsible for the decomposition of Indigo carmine.



## REFERENCES

- [1] Baban, A.; Yediler, A. & Ciliz, N.K., (2010). Integrated water management and CP implementation for wool and textile blend process. *Clean*. 38(1): 84-90.
- [2] Robinson, T.; McMullan, G; Marchant, R. & Nigam, P., (2001). Remediation of dyes in textile effluent: a critical review on current treatment technologies with a proposed alternative. *Bioresource Technology*. 77: 247-255.
- [3] Solomon P.A., Basha C.A., Ramamurthi V., Koteeswaran K. & Balasubramanian N., (2009). Electrochemical degradation of Remazol Black B dye effluent. *Clean*. 37(11): 889-900.
- [4] Fujishima, A., Zhang, X. & Tryk, D.A., (2008). TiO<sub>2</sub> photocatalysis and related surface phenomena. *Surf. Sci. Rep.* 63: 515-582.
- [5] Linsebigler, A.L., Lu, G.Q. & Yates, J.T., (1995). Photocatalysis on TiO<sub>2</sub> surfaces principles, mechanisms, and selected results. *Chem. Rev.* 95: 735-758.
- [6] Henderson, M.A., (2011). A surface science perspective on TiO<sub>2</sub> photocatalysis *Surf. Sci. Rep.* 66: 185-297.
- [7] Ohno, T., Sarukawa, K., Tokieda K. & Matsumura M., (2001). Morphology of a TiO<sub>2</sub> photocatalyst (Degussa, P-25) consists of anatase and rutile crystalline phases. *J. Catal.* 203: 82-86.
- [8] Dutta P.K., Dutta J., Tripathi V.S., (2004). Chitin and chitosan: chemistry, properties and applications. *J. Sci. Ind. Res. India*. 63(1): 20-31
- [9] Rinaudo M., (2006). Chitin and chitosan: properties and applications. *Prog. Polym. Sci.* 31(7): 603-632.
- [10] Kim I.Y., Seo S.J., Moon H.S., Yoo M.K., Park I.Y., Kim B.C., Cho C.S., (2008). Chitosan and its derivatives for tissue engineering applications. *Biotechnol. Adv.* 26(1): 1-21.
- [11] Mati-Baouche N., Elchinger P.H., H. de Baynast, Pierre G., Delattre C., Michaud P., (2014). Chitosan as an adhesive. *Eur. Polym. J.* 60: 198-212.
- [12] Borney A., Teissedre P.L., (2005). Applications and interest of chitin, chitosan and their derivatives in enology. *J. Int. Sci. Vigne. Vin.* 39(4): 199-207.

[13] Santos Menegucci J.D., Santos M.K.M.H., Dias D.J.S., Chaker J.A., Sousa M.H., (2015). One-step synthesis of magnetic chitosan for controlled release of 5-hydroxytryptophan. *J. Magn. Mater.* 380: 117-124.

[14] Cai Y., Lapitsky Y., (2014). Formation and dissolution of chitosan/pyrophosphate nanoparticles: is the ionic crosslinking of chitosan reversible?. *Colloid Surf B.* 115: 100-108.

[15] Dowling M.B., Kumar R., Keibler M.A., Hess J.R., Bochicchio G.V., Raghavan S.R., (2011). A self-assembling hydrophobically modified chitosan capable of reversible hemostatic action. *Biomaterial.* 32(13): 3351-3357.

[16] Butstraen C., Salaün F., (2014). Preparation of micro capsules by complex coacervation of gum Arabic acid and chitosan. *Carbohydr. Polym.* 99: 608-616.

[17] Martins A.F., D.M. de Oliveira, A.G.B. Pereira, E.C. Muniz., (2012). Chitosan/TPP microparticles obtained by microemulsion method applied in controlled release of heparin. *Int. J. Biol. Macromol.* 51(5): 1127-1133.

[18] Apana K., Dhanya A., (2016). Synthesis and Evaluation of TiO<sub>2</sub>/Chitosan based hydrogel for the adsorptional photocatalytic degradation of azo and anthraquinone dye under UV light irradiation. *Procedia Technology.* 24: 611-618.

[19] B. Hastuti, A. Masykur, S. Hadi., (2016). Modification of chitosan by swelling and crosslinking using epichlorohydrin as heavy metal Cr (VI) adsorbent in batik industry wastes. *IOP Conf. Series: Materials Science and Engineering.* 107.

[20] Chang Y, Huang C, Hsu W and Chang F., (2006). Removal of Hg<sup>2+</sup> from aqueous solution using alginate gel containing chitosan. *J. Appl. Polym. Sci.* 104: 2866-2905.

[21] Chen X, Liu J, Feng Z and Shao, (2005). Macroporous chitosan/carboxymethylcellulose blend membranes and their application for lysozyme adsorption. *J. Apply. Polym. Sci.* 96: 1267-1274.

[22] Wang A., Wang L. and Sun S., (2005). Adsorption properties of crosslinked carboxymethyl-chitosan resin with Pb(II) as template ions. *Journal of Hazardous Material.* 136: 930-937.

[23] Katarina R K, Takayanagi T, Oshita K, Oshima M and Motomizu S., (2008). Sample Pretreatment Using Chitosan-based Chelating Resin for the Determination of Trace Metals in Seawater Samples by Inductively Coupled Plasma-Mass Spectrometry. *J. Anal. Sci.* 24: 1537-1544.

[24] Oshita K, Takayanagi T, Oshima M and Motomizu S., (2008). Adsorption Properties of Ionic Species on Cross-linked Chitosans Modified with Catechol and Salicylic Acid Moieties. *J. Anal. Sci.* 24: 665-668.

[25] Masykur A., Santosa S.J., Siswanta D. and Jumina, (2014). Grafting of Chloroacetic Acid on EGDE Cross-Linked Chitosan to Enhance Stability and Adsorption Capacity For Pb(II) Ions. *Indo. J. Chem.* 14: 63-70.

[26] Chen C.Y., Yang C.Y. and Chen A.H., (2011). Biosorption of Cu(II), Zn(II), Ni(II) and Pb(II) ions by cross-linked metal-imprinted chitosans with epichlorohydrin. *Journal of Environmental Management.* 92: 796-802.

[27] Pirkanniemi K. and Sillanpää M., (2002). Heterogeneous water phases catalysis as an environmental application: a review. *Chemosphere.* 48(10): 1047-1060.

[28] Stylidi M., Kondarides D.I. and Verykios X.E., (2004). Visible light-induced photocatalytic degradation of Acid Orange 7 in aqueous TiO<sub>2</sub> suspensions. *Applied Catalysis B: Environmental.* 47(3): 189-201.

[29] Kaur S. and Singh V., (2007). TiO<sub>2</sub> mediated photocatalytic degradation studies of Reactive Red 198 by UV irradiation. *Journal of Hazardous Materials.* 141(1): 230-236.

[30] Kormann C., Bahnemann D. and Hoffmann M.R., (1991). Photolysis of chloroform and other organic molecules in aqueous titanium dioxide suspensions. *Environ. Sci. Technol.* 25(3): 494-500.

[31] Liu W., Chen S., Zhao W. and Zhang S., (2009). Study on the photocatalytic degradation of trichlorfon in suspension of titanium dioxide. *Desalination.* 249(3): 1288-1293.



[32] Peralta-Hernández J.M., Meas-Vong Y., Rodríguez F.J., Chapman T.W., Maldonado M.I. and Godínez L.A., (2006). In situ electrochemical and photoelectrochemical generation of the fenton reagent: A potentially important new water treatment technology. *Water Res.* 40(9): 1754-1762.

[33] Lakshmi S., Renganathan R. and Fujita S., (1995). Study on TiO<sub>2</sub>-mediated photocatalytic degradation of methylene blue. *Journal of Photochemistry and Photobiology A: Chemistry.* 88(2-3): 163-167.

[34] Hurum D.C., Agrios A.G., Gray K.A., Rajh T. and Thurnauer M.C., (2003). Explaining the enhanced photocatalytic activity of Degussa P25 mixed-phase TiO<sub>2</sub> using EPR. *J. Phys. Chem. B.* 107(19): 4545– 4549.

[35] Muhammad Amtiaz Nadeem et al., (2014). Principles and mechanisms of photocatalytic dye degradation on TiO<sub>2</sub> based photocatalysts: a comparative overview, *RSC Advances.* 4: 37003-37026.

[36] Raji C., Anirudhan T.S., (1998). Batch Cr(VI) removal by polyacrylamide-grafted sawdust: Kinetics and thermodynamics, *Water Res.* 32: 3772-3780.

[37] Goyal N., Jain S.C., Banerjee U.C., (2003). Comparative studies on the microbial adsorption of heavy metals, *Adv. Environ. Res.* 7: 311-319.

[38] Yang T.C., Zall R.R., (1984). Absorption of metals by natural polymers generated from seafood processing wastes. *Ind. Eng. Chem. Prod. Res. Dev.* 23: 168– 172.

[39] Dalia Khalid Mahmoud, Mohamad Amran Mohd Salleh, Wan Azlina Wan Abdul Karim. (2012). Langmuir model application on solid-liquid adsorption using agricultural wastes: Environmental application review. *Journal of Purity, Utility Reaction and Environment.* 1(4): 170-199

[40] Irving Langmuir. (1918). The adsorption of gases on plane surfaces of glass, mica and platinum. *J. Am. Chem. Soc.* 40(9): 1361–1403

[41] Sing et al. (1985). Reporting physisorption data for gas/solid systems with special reference to the determination of surface area and porosity. *Pure and Applied Chemistry.* 57: 603-619

[42] Hudec, P. (2012). Texture of solid materials. Characterization of adsorbents and catalysts via physical nitrogen adsorption. Bratislava, Slovakia: STU (in Slovak)

[43] Lecloux, A.J. (1981). Texture of catalysts. In J. R. Anderson, & M. Boudart (Eds.). Catalyst: Science and technology. 2: 171-230

[44] Thomas, J.M. & Thomas, W.J. (1997). Principles and practice of heterogeneous catalyst. Weinheim, Germany: VCH.

[45] Campos, R., Kandelbauer, A., Robra, K., Cavaco-Paulo, A. and Gübitz, G.M. (2001) Indigo Degradation with Purified Laccases from *Trametes hirsuta* and *Sclerotium rolfsii*. *Journal of Biotechnology*. 89: 131-139.

[46] Elba Ortiz et al. (2016), Degradation of indigo carmine using advanced oxidation processes: Synergy effects and toxicological study. *Journal Environmental Protection*. 7: 1693-1706

[47] Enrico Mendes Saggiaro et al. (2011). Use of titanium dioxide photocatalysis on the remediation of model textile wastewaters containing azo dye. *Molecules*. 16: 10370-10386

[48] Fozia Z. Haque, Ruchi Nandanwar and Purnima Singh. (2017). Evaluating photodegradation properties of anatase and rutile TiO<sub>2</sub> nanoparticles for organic compounds. *Optik*. 128: 191-200

[49] M.Z.B. Mukhlis et al. (2013). Photocatalytic degradation of different dyes using TiO<sub>2</sub> with high surface area: A kinetic study. *J. Sci. Res.* 5(2): 301-314

[50] Y.A. Aydin, N.D. Aksoy, (2009). Adsorption of chromium on chitosan: optimization, kinetics and thermodynamics, *Chem. Eng. J.*, 151: 188-194

[51] A. Mittal, L. Krishnan, V.K. Gupta, (2005). Removal and recovery of malachite green from wastewater using an agricultural waste material, de-oiled soya, *Sep. Purif. Technol.* 43: 125-133

[52] Gordon McKay, Len Foong Koong, Koon Fung Lam and John Barford, (2013). A comparative study on selective adsorption of metal ions using aminated adsorbents. *Journal of Colloid and Interface Science*. 395: 230-240

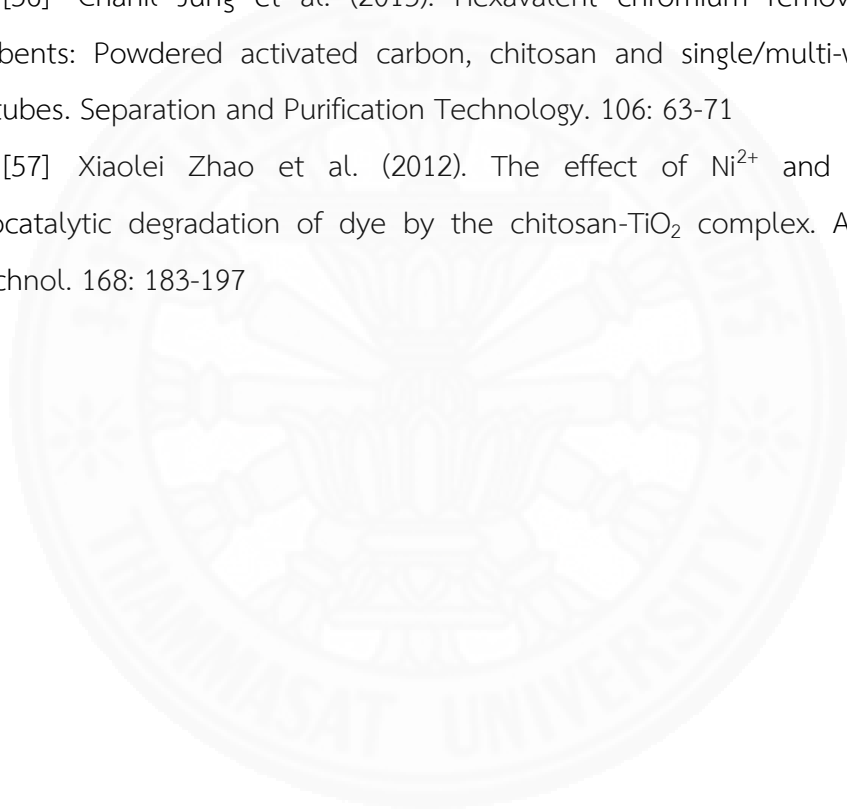
[53] Laus R., Costa T.G., Szpoganicz B., Fávere V.T., (2010). Adsorption and desorption of Cu(II), Cd(II), Pb(II) ions using chitosan crosslinked with epichlorohydrin-triphosphate as the adsorbent. *Journal of Hazardous Materials*. 183: 233-241.

[54] W. S. Wan Ngah et al. (2006). Adsorption of chromium from aqueous solution using chitosan beads. *Adsorption*. 12: 249-257

[55] Şenay Hamarat Baysal et al. (2006). Comparative studies on the adsorption of Cr(VI) ions on to various sorbents. *Bioresource Technology*. 98: 661-665

[56] Chanil Jung et al. (2013). Hexavalent chromium removal by various adsorbents: Powdered activated carbon, chitosan and single/multi-walled carbon nanotubes. *Separation and Purification Technology*. 106: 63-71

[57] Xiaolei Zhao et al. (2012). The effect of Ni<sup>2+</sup> and Cu<sup>2+</sup> on the photocatalytic degradation of dye by the chitosan-TiO<sub>2</sub> complex. *Appl. Biochem. Biotechnol*. 168: 183-197



**BIOGRAPHY**

Name	Mr. Thunpichet Oonesirithapsakul
Date of Birth	December 7, 1990
Educational Attainment	2012: B. Sc. (Chemistry), Department of Chemistry, Faculty of Science, Chandrakasem Rajabhat University
Scholarship	2013: Research Professional Development Project under the Science Achievement Scholarship of Thailand (SAST)
Publications	Oonesirithapsakul T., Plucktaveesak N. (2017). Fabrication and characterization of TiO <sub>2</sub> embedded chitosan microbeads with multifunctional properties, <i>MRS Thailand 2017 E-proceeding</i> . Poster presented at The First Materials Research Society of Thailand International Conference, Chiangmai, Thailand, 31 <sup>st</sup> October – 3 <sup>rd</sup> November (pp. 443-449)